

# In situ Functionalized Mesoporous Silicas for Sustainable Remediation Strategies in Removal of Inorganic Pollutants from Contaminated Environmental Water

Natalia G. Kobylinska,\* Vadim G. Kessler, Gulaim A. Seisenbaeva, and Oksana A. Dudarko

Cite This: *ACS Omega* 2022, 7, 23576–23590

Read Online

ACCESS |

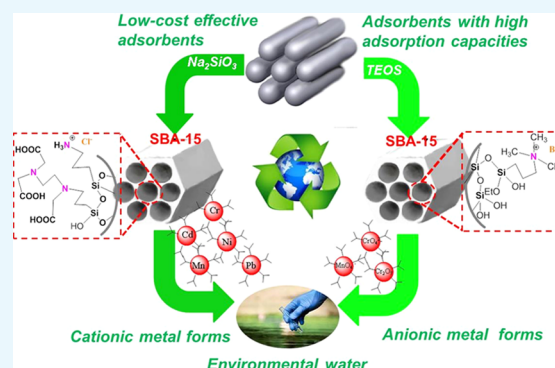
Metrics &amp; More

Article Recommendations

Supporting Information

**ABSTRACT:** Low-cost mesoporous silicas of the SBA-15 family were prepared, aimed for removal of a broad spectrum of both cationic and anionic forms of hazardous metal pollutants (Cr(III, VI), Mn(II, VII), Pb(II), Cd(II), and Cu(II)) from environmental water. Series of mono- and bifunctional materials with immobilized ethylenediaminetriacetic acid (EDTA), primary amine ( $\text{NH}_2$ ), and quaternary ammonium (QAS) groups were prepared in a cost-efficient one-step synthesis using two silica sources, low-cost sodium metasilicate ( $\text{Na}_2\text{SiO}_3 \cdot 9\text{H}_2\text{O}$ ) and the conventional source—tetraethylorthosilicate (TEOS). The functionalized SBA-15 samples obtained from both silica sources were highly ordered, as evidenced by TEM and SAXS data. All obtained materials were mesoporous with high surface area values of up to  $745 \text{ m}^2/\text{g}$ , pore volumes from  $0.99$  to  $1.44 \text{ cm}^3/\text{g}$ , and narrow pore distributions near  $7 \text{ nm}$ .

The adsorption affinity of the EDTA-functionalized samples followed the common order  $\text{Pb(II)} > \text{Cd(II)} > \text{Cu(II)} > \text{Cr(III)} > \text{Mn(II)}$ , which could be explained based on the Pearson theory. The highest adsorption capacities were observed for samples functionalized by EDTA groups using TEOS for synthesis (TEOS/EDTA):  $195.6 \text{ mg/g}$  for Pb(II),  $111.2 \text{ mg/g}$  for Cd(II),  $58.7 \text{ mg/g}$  for Cu(II),  $57.7 \text{ mg/g}$  for Cr(III), and  $49.4 \text{ mg/g}$  for Mn(II). Moreover, organic matter (humic acid up to  $10 \text{ mg/L}$ ) and inorganic (Na(I), K(I), Mg(II), Ca(II), etc) macrocomponents present in environmental water had almost negligible effect on the removal of these cations. The NaSi/EDTA/ $\text{NH}_2$  sample revealed a better selectivity compared to the NaSi/ $\text{NH}_2$  sample towards such species as Cr(III), Mn(II), Cd(II), and Cu(II). The chromate-ions uptake at pH 7.5 by the TEOS/QAS sample turned practically unaffected by the presence of doubly charged anions ( $\text{CO}_3^{2-}$ ,  $\text{SO}_4^{2-}$ ). The content of functional groups on the surface of MS decreased only slightly ( $\sim 1$ – $5\%$ ) after several regeneration cycles. The complete desorption of all heavy metal ions can be achieved using  $1 \text{ mol/L}$  EDTA solution. Reusability tests demonstrated the complete stability of the adsorbent for at least five to six consecutive adsorption/desorption cycles with no decrease in its adsorption characteristics compared to those obtained by  $0.05 \text{ mol/L}$   $\text{HNO}_3$  treatments. The synthesized mesoporous materials were evaluated for removal of the heavy metal ions from drinking and different natural water samples, proving their potential as sustainable, effective, and cost-efficient adsorbents.



## 1. INTRODUCTION

Access to clean water is a prerequisite for human life. Environmental pollution represents a serious threat to human health, natural resources, and ecological systems. The ongoing climate change, associated with warmer weather and irregular acidic atmospheric precipitation, leads to acidification and increased dissolution of mineral components, resulting in increased release of heavy metals. They are recognized as the dominant class of hazardous pollutants, because of long retention times in soil and water and the challenges they cause to the environment.<sup>1</sup>

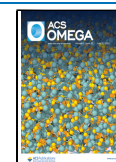
Extensive research has produced various approaches to heavy metal removal from environmental and wastewaters, including reverse osmosis, electrodialysis,<sup>2</sup> chemical precipitation,<sup>3</sup> ion exchange,<sup>4</sup> adsorption,<sup>5</sup> membrane filtration,<sup>6</sup> coagulation–flocculation,<sup>7</sup> cloud point extraction,<sup>8</sup> flotation, and electro-

chemical technologies. Adsorption is a very effective technique and is considered to be superior to other technologies for water treatment in terms of initial cost, simplicity of design, ease of process, and stability to toxic substances.<sup>5</sup> Adsorptive processes become uneconomical only in case of rather high concentrations of pollutants in solution. Although adsorption technologies are well established, a significant limitation is posed by the cost of the adsorbent materials. Many kinds of adsorbents for heavy metals' removal have been studied, such as activated carbons,

Received: April 6, 2022

Accepted: June 17, 2022

Published: July 1, 2022



various nanomaterials,<sup>10</sup> including iron-based metal oxides,<sup>11</sup> metal-organic frameworks,<sup>12</sup> polymeric and biomass-based materials,<sup>13</sup> metal phosphates,<sup>14</sup> etc. Compared to them, oxide-based mineral matrices possess a number of advantages. One can mention, in particular, the greater stability of such materials in aggressive media, and when exposed to intense radiation, along with thermal stability.<sup>15,16</sup> Nevertheless, only a few adsorbents are broadly used in everyday practice. The challenging requirements for industrial adsorbents include such parameters as high selectivity for heavy metal ions, easy desorption of metal ions, high adsorption/desorption rates, high adsorption capacity, durability in repeated use, low cost, and high mechanical stability. Carbon and silica-based materials are being increasingly used, while increased-selectivity and better-capacity materials are still required.

Hybrid organic-inorganic functionalized mesoporous materials, including those based on silica, started to attract serious attention since the 1990s.<sup>17</sup> Easy control of the pore sizes of these materials is very attractive because pores greater than 7 nm are generally required for efficient separation and good mass transport between liquid and solid phases.<sup>18</sup> Covalent bonding between an organic functional component and the mineral carrier is considered as a more potential grafting strategy for reusable adsorbents because it offers hydrolytic stability.<sup>19</sup> The most promising methods for obtaining such materials are “one-pot” synthesis<sup>20,21</sup> and post-synthesis grafting methods.<sup>22</sup> The removal of heavy metal ions by various functionalized mesoporous silica families (M41S, MCM-*n*, SBA-*n*, FDU-*n*, KIT-*n*) has been extensively reviewed in several recent reports.<sup>16,23</sup> Use of different types of N-containing functional groups is a promising route for functionalization of the silica surface to boost its effectiveness in removal of metal ions. Functional groups, such as heterocyclic<sup>24</sup> or aminopropyl<sup>22</sup> groups, have been grafted on the mesoporous silica for removal of Cr(VI) ions. Li and co-authors<sup>22</sup> reported the maximum adsorption capacity of aminopropyl-SBA-15 to reach 405 mg/g at pH = 2. In this case, the electrostatic interaction between the positively charged adsorbent and the anionic adsorbate played an important role. SBA-15 functionalized with a bis-pyrazole ligand for removal of Cr(III) revealed a maximum adsorption capacity of up to 1.4 mmol/g (72.5 mg/g) at pH 6.0, while it almost did not adsorb Cr(VI).<sup>24</sup> MCM-41 and MCM-48 modified with *N,N* dimethyldodecylamine and dodecylamine<sup>25</sup> were prepared and studied for selective metal ion adsorption. The adsorption capacity of MCM-41 modified with dimethyldodecylamine (210 mg/g for Cu<sup>2+</sup>) was found to be higher than for the one grafted with dodecylamine. The uptake order for single- and multicomponent solutions was Cu<sup>2+</sup> > Pb<sup>2+</sup> > Cd<sup>2+</sup> > Co<sup>2+</sup>. Gupta and co-authors<sup>26</sup> proposed the removal of toxic metal ions (e.g., Pb(II), Hg(II), and Cd(II)) from aqueous solutions using guanine-functionalized microporous SBA-16 with a maximum adsorption capacity of 289.9 mg/ for Pb(II), 259.9 mg g<sup>-1</sup> for Hg(II), and 228.8 mg/g for Cd(II). Faghian and co-workers<sup>27</sup> used MCM-41 and MCM-48 functionalized with [amino-ethylamino]-propyl-trimethoxysilane for the heavy metal extraction. The adsorption capacity of MCM-41 was higher than that of MCM-48, because the aminopropyl groups inside pores with larger dimensions had more freedom and better accessibility to metal ions. This ability for metal ion adsorption was attributed to its using a larger pores-containing material from the mesoporous family, such as SBA-15 (3–30 nm<sup>28</sup>) or HMS.<sup>29</sup> The uptake order for the studied ions was Co(II) (103.09 mg/g) > Cu(II) (172.41 mg/g) > Pb(II)

(169.49 mg/g) > Cd(II) (64.93 mg/g), in agreement with the stability of the M–N coordination bond. In another work,<sup>30</sup> greatly improved adsorption using amino-functionalized adsorbents with a high concentration of functional groups was demonstrated. The glycine-functionalized mesoporous silica particles could remove up to 2.81 mmol/g of Co(II) ions or 3.02 mmol/g of Ni(II) ions from aqueous solution, a capacity that is tenfold higher than that of unmodified silica.<sup>31</sup>

Adsorptive materials functionalized by chelating ligands such as amino poly-carboxylates<sup>32</sup> including EDTA were more efficient than other adsorbents for efficient extraction of heavy metal ions.<sup>33,34</sup> Actually, formation of the multifunctional surface layers is an effective tool for a more subtle tailoring of the properties of silicas, in particular, sorption capacity. This is due to the emerging possibility of varying both the nature and the ratio of functional groups on the surface. This could be achieved easily in the course of the synthesis by varying the ratio of the functional silanes, and changing the nature of the reaction medium or the order of addition of reagents in the reaction mixture. One needs also to take into account the possible effect of the mutual influence of the functional groups present in the surface layers, which can provide synergistic effects.<sup>35</sup> Pandey reported<sup>36</sup> that polyfunctional sorbents were found suitable for treatment of real wastewaters containing heavy metal ions. Finally, in our previous work,<sup>37</sup> a series of effective bifunctional mesoporous silicas were prepared for removal of rare earth elements and heavy metal ions from aqueous solutions under noncompetitive conditions. Adsorption isotherms and regeneration studies suggested that the prepared EDTA-based mesoporous silica could be used as an effective and reusable adsorbent with good kinetic features in heavy metal-removing processes. Based on our literature review, the main disadvantage of materials with mesoporous structure in this context was the cost of their synthesis.<sup>38</sup> Adsorption onto cost-effective mesoporous materials would be economically favorable and straightforward and the ultimately good scenario.

The aim of this work was to trace approaches to obtain sustainable mesoporous SBA-type adsorbent materials with broad functionality, exploiting both anionic, such as ethylenediaminetriacetate (EDTA), potential complex-binding ligand functions, such as that of a primary amine (NH<sub>2</sub>), and cationic quaternary ammonium (QAS) ones. For this purpose, aiming at improved cost efficiency, the optimizations of the one-pot syntheses of functionalized SBA-15 silica were performed starting either from cost-efficient sodium metasilicate or from conventional TEOS as silica sources. Changing the coordination environment and steric accessibility of nitrogen atoms in the functional groups and their concentration permitted identification of the optimal conditions in adsorbent preparation for selective extraction of the Cr(III, VI), Mn(II, VII), Pb(II), Cd(II), and Cu(II) species. Material regeneration with preservation of the main textural parameters (surface area, concentration of functional groups, etc.) was also investigated in detail as a factor to reduce the costs of adsorbents for water treatment. Finally, a comparative study of the synthesized mesoporous silicas as adsorbents in the removal of heavy metals from drinking and environmental water was carried out, evaluating the potential interference from macrocomponents of polluted waters.

## 2. MATERIALS AND METHODS

**2.1. Reagents.** Aminopropyltriethoxysilane ((C<sub>2</sub>H<sub>5</sub>O)<sub>3</sub>Si-(CH<sub>2</sub>)<sub>3</sub>NH<sub>2</sub>, APTES, 98%), 3-aminopropylsilanetriol

((HO)<sub>3</sub>Si(CH<sub>2</sub>)<sub>3</sub>NH<sub>2</sub>, APTS, Gelest (22–25% in water)), trisodium salt of *N*-(triethoxysilylpropyl) ethylenediaminetriacetic acid ((C<sub>2</sub>H<sub>5</sub>O)<sub>3</sub>Si(CH<sub>2</sub>)<sub>3</sub>N(CH<sub>2</sub>CO<sub>2</sub>Na)CH<sub>2</sub>CH<sub>2</sub>N(CH<sub>2</sub>CO<sub>2</sub>Na)<sub>2</sub>, TMS-EDTA, 40% in water), ethylenediaminetetraacetic acid disodium salt (EDTANa<sub>2</sub>, ACS reagent, 99.0–101.0%), sodium metasilicate (Na<sub>2</sub>SiO<sub>3</sub>·9H<sub>2</sub>O, SS), and Pluronic P123 (Merck, MW ~5800) were obtained from Sigma-Aldrich. Tetraethoxysilane (TEOS, 99%) and trimethyl[3-(trimethoxysilyl)propyl]ammonium chloride (ca. 50% in Methanol) (ATMTES, 55%) were obtained from Fluorochem.

ICP multielement standard solution IV CertiPUR Merck (Supelco) for 23 elements with a concentration of 1000 mg/L (in nitric acid) was used.

All used chemicals were of analytical grade without additional purification. The Cu(II), Fe(III), Cd(II), Cr(III, VI), Mn(II, VII) and Pb(II) solutions were prepared by direct dissolution of proper amounts of Cu(NO<sub>3</sub>)<sub>2</sub>·5H<sub>2</sub>O, Fe(NO<sub>3</sub>)<sub>3</sub>·9H<sub>2</sub>O, Cd(NO<sub>3</sub>)<sub>2</sub>·4H<sub>2</sub>O, Cr(NO<sub>3</sub>)<sub>3</sub>·9H<sub>2</sub>O (99,99%), K<sub>2</sub>CrO<sub>4</sub> (99,9%), Mn(NO<sub>3</sub>)<sub>2</sub>·6H<sub>2</sub>O, KMnO<sub>4</sub> (99,97%) and Pb(NO<sub>3</sub>)<sub>2</sub> (99,0%) salts, respectively. All stock and working solutions were prepared using deionized water (18.2 MΩ/cm) from Milli-Q System (Millipore, France).

**2.2. Synthesis of Adsorbents.** The preparation of SBA-15 functionalized with quaternary ammonium groups (TEOS/QAS) and EDTA groups (denoted as TEOS/EDTA) was similar to the hydrothermal method reported by Zhao et al. using TEOS as the silica source and Pluronic P123 as a corresponding structure-directing template.<sup>20,21</sup>

**2.2.1. Synthesis of TEOS/QAS.** Briefly, 4 g of triblock copolymer P123 was stirred with 20 mL of deionized water at 35 °C until fully dissolved (clear solution), followed by adding 20 mL of HCl (37 wt %) and dropwise addition of 10 mL of TEOS and ATMTES mixture (with a ratio of ATMTES/TEOS = 1:2). The mixture was allowed to stir at 40 °C for 24 h before transferring into a Teflon-sealed bottle in an autoclave, which was then heated to 100 °C for 1 day in an oven without stirring. The solid was filtered off, washed three times with ethanol/water mixture in a Soxhlet apparatus to remove the template, and then washed with deionized water. The resulting solid was vacuum-dried at 110 °C.

**2.2.2. Synthesis of TEOS/EDTA.** Generally, surfactant P123 (4 g) was dissolved in 20.0 mL of HCl (37 wt %) and 10.8 mL of deionized water was added during 3.5 h under rapid stirring at 40 °C. Next, 4.4 mL (0.02 mmol) of TEOS was added dropwise under stirring to the sol solution at 40 °C. After half an hour, about 10 mL of TMS-EDTA solution in methanol (1:1) was added to the synthesized gel and stirred for 24 h at 50 °C in hydrothermal condition without stirring. The precipitate was separated and washed using ethanol/HCl (1:1) solution several times. TEOS/EDTA was decanted and washed with deionized water until reaching the neutral pH, and thereafter dried under vacuum at 110 °C.

For preparation of SBA-15 functionalized aminopropyl groups (NaSi/NH<sub>2</sub>) and its bifunctional derivate with EDTA groups (NaSi/EDTA/NH<sub>2</sub>), the template method was used with sodium metasilicate as the silica source.<sup>18</sup>

**2.2.3. Synthesis of NaSi/NH<sub>2</sub>.** 3.2 g of surfactant was dissolved in a mixture of 2 M HCl (62 mL) with constant stirring for 30 min at room temperature. Then, APTES (0.0016 mol) was added to the template solution with stirring for 30 min; 0.016 mol of SS separately dissolved in 32 mL of water was added in a thin stream to the resulting clear mixture. Sedimentation began immediately and ended after about 5

min. The resulting heterogeneous system was further stirred for 2 h at 40 °C. Then, hydrothermal treatment (HTT) was performed at 80 °C for 20 h, followed by filtration of the white precipitate. This precipitate was dried in air overnight. After that, boiling in acidified ethanol four times with stirring for 3 h was done for template removal. The obtained solid was dried for several hours at 50 °C, and then dried in vacuum for 3 h at 110 °C.

**2.2.4. Synthesis of NaSi/EDTA/NH<sub>2</sub>.** Pluronic 123 (4 g) was dissolved in 2 M HCl (72 mL) with constant magnetic stirring (30 min) at room temperature. Then, equimolar amounts of EDTA and APTES (0.002 mol) were added at room temperature. Simultaneously, the SS was separately dissolved in 40 mL of water. To obtain the mixture, 0.04 mol of SS was added in a thin stream. The resulting clear mixture was observed. The subsequent operations were the same as for NaSi/NH<sub>2</sub>.

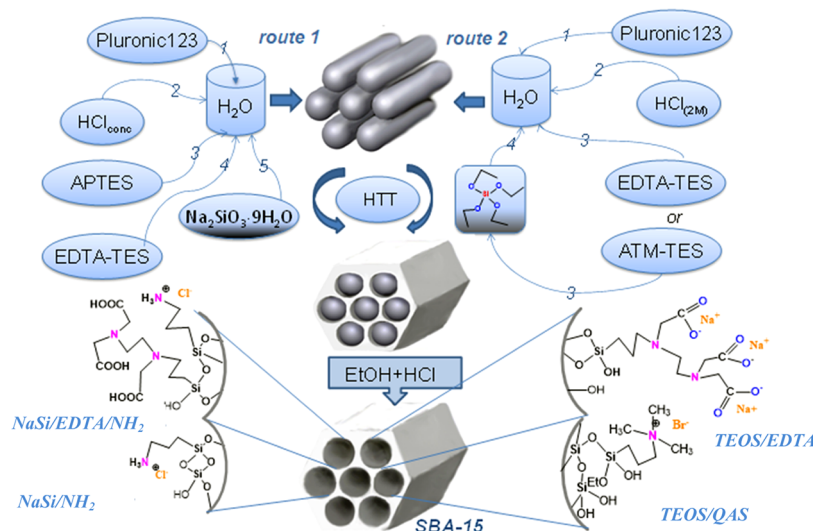
**2.3. Characterization.** Small-angle X-ray scattering (SAXS) patterns were obtained using DRON-4-07 diffractometer (Cu Kα) radiation, (λ = 1.5418 Å) in the small-angle range (2θ = 0.5–5.0). Fourier transform infrared spectra (FTIR) of all samples were recorded using tablets with KBr (1:10) on a Nicolet NEXUS 470 spectrophotometer in the range 400–4000 cm<sup>-1</sup>. In all cases, 50 scans with a resolution of 4 cm<sup>-1</sup> were applied.

The Hitachi TM-3000 and JSM-6100 (JEOL, Japan) scanning electron microscopes were used for morphology evaluation. Transmission electron microscopy images were measured using JEM-1230 and JEM-2100F (JEOL, Japan) apparatuses. The textural parameters of the mesoporous materials were studied using the N<sub>2</sub> adsorption/desorption isotherms recorded at 77 K with a Kelvin-1042 apparatus (Costech Instruments). The samples were initially degassed in a helium flow at 110 °C for 1 h under vacuum (10<sup>-4</sup> mbar). The specific surface area (S<sub>BET</sub>) of the obtained mesoporous samples was determined by the Brunauer–Emmet–Teller (BET) method.<sup>39</sup> The pore sizes and their distributions were calculated from the desorption branches of the corresponding N<sub>2</sub> isotherm using the Barrett, Joyner, and Halenda (BJH) method.<sup>40</sup>

Concentrations of the available functional groups on the SBA-15-based solids were determined using various types of potentiometric titration. Acid–base titration (direct): A series of the sample with protolytically active groups (~0.05 g) was poured into 25 mL of 0.1 M NaNO<sub>3</sub>, incubated for 24 h, and titrated with 0.1 M NaOH solution. Acid–base titration (back): The solid (~0.05 g) was placed in a flask, 20 mL of 0.1 M NaNO<sub>3</sub> solution was added, and then 3–5 mL of 0.1 M NaOH solution was added to adjust the pH of the solution to 9. The mixture was shaken overnight. This solution was stirred magnetically, and titrated with 0.05 M HCl until a pH change to 2.5 was observed. Each measurement was repeated 3 times, to obtain the mean value of the functional group content in the sorbent by treating the data similarly to the data of direct titration.

A flame atomic absorption spectrometer (AAS) equipped with fast sequential mode (ICE 3500, Thermo Scientific, USA) using the acetylene-air flame was applied. Calibration curves were obtained from 0.015 to 0.50 mg/L for Cd, Co, Cu, Mn, Cr, and Zn; from 1.5 to 15.0 mg/L for Fe; from 0.2 to 2.5 mg/L for Mg; and from 0.1 to 2.0 mg/L for Pb.

**2.4. Batch (Static) Adsorption Experiments.** The affinity of the adsorbents toward metal ions was initially probed in static experiments. Fifty milligrams of the test sample was shaken at 220 ppm with 25 mL solutions of salts of the corresponding

Scheme 1. Synthetic Routes for Preparation of the Functionalized Mesoporous SBA-15 Samples<sup>a</sup>

<sup>a</sup>We chose chelating and ion-exchange functional groups for one-pot synthesis of SBA-based adsorbents by acidic hydrolysis of both silica sources, namely (1) ethylenediaminetriacetic acid groups (TEOS/EDTA); (2) ammonium trimethylpropyl bromide groups (TEOS/QAS); (3) protonated primary aminopropyl groups (NaSi/NH<sub>2</sub>); (4) polyfunctional sample with a combination of chelating and ion-exchange groups – ethylenediaminetriacetic and aminopropyl groups (NaSi/EDTA/NH<sub>2</sub>).

metal ions. The initial metal concentration was maintained around 30–50 mg/L, with pH<sub>initial</sub> values varying between 2 and 8. Subsequent filtration of the suspension was performed using a membrane filter (nylon, 0.2 mm). The concentration of metal ions was determined in the supernatant by AAS, by diluting to the linear range of the calibration curve for each metal. Each experiment was carried out at least three times.

The maximum adsorption capacity ( $q_e$ ) and distribution coefficient ( $K_d$ ) were determined as follows

$$q_e (\text{mg/g}) = (C_0 - C_e) \cdot V \cdot A_r / m$$

$$K_d (\text{mL/g}) = \frac{(C_0 - C_e) \cdot V}{C_e \cdot m}$$

where  $C_0$  and  $C_e$  (mg/L) are the initial and equilibrium metal ion concentrations, respectively;  $V$  (mL) is the solution volume;  $A_r$  is the atomic mass; and  $m$  (g) is the weight of the mesoporous adsorbent.

**2.5. Competitive Adsorption of Metal Ions.** 0.5 mL of the ICP multielement standard solution was added to a 100 mL volumetric flask and diluted with deionization water. Fifty milligrams of the adsorbent was mixed with 100 mL of freshly prepared solution (pH 6.0) and shaken for 30 min at room temperature. After filtration of the adsorbent from the liquid, desorption of metals from the sorbent was carried out. For this purpose, 5.0 mL of 0.1 mol/L HNO<sub>3</sub> was added to the adsorbent, the mixture was shaken for 30 min, and the adsorbent was separated by centrifugation. The resulting acidic supernatant solution was analyzed by AAS.

The presented procedure was tried on the modeling solutions (the stock solution was diluted to 5  $\mu\text{g/L}$  with deionized water). An aliquot of modeling solution, containing a mixture of ions in the analyte, was transferred into a beaker and left at room temperature for 15 min with the added adsorbents (50 mg).

**2.6. Regeneration of Sorbents and Desorption Conditions.** To evaluate the reusability of the obtained adsorbents, various cycles of adsorption/desorption of heavy metal ions were performed. Desorption tests for materials after

adsorption were performed using three solutions, HCl (0.05–1.0 mol/L), HNO<sub>3</sub> (0.05–1.0 mol/L), and EDTA (1.0–2.0 mol/L), in static and dynamic conditions. In static condition experiments, the sorbent samples with a known amount of the adsorbed metal were placed in the flasks and shaken for 3–12 h with 5 mL of desorbing agent solutions at 22 °C. After that, the metal concentrations in the solutions were measured by AAS.

Desorption experiments in dynamic condition: Briefly, a solution of HNO<sub>3</sub> (0.05 mol/L) was passed through a column with  $\varnothing$  8 mm and adsorbent layer height near 10 mm using a peristaltic pump at the rate of 1 mL/min.

**2.7. Environmental Water Sample Assay.** The real environmental samples, including artesian, urban river, and lake water, were collected during December 2020 - December 2021 from Kyiv (Ukraine), an artesian well (50 meters deep) in Schevchenko Park (city district area), Dnipro River (center of the city), and Verchovina Lake (near the incineration plant). For preserving, 1 mL aliquots of 68% nitric acid per 1 L of the water samples were added. All water samples were filtered through a 0.45  $\mu\text{m}$  size Millipore membrane filter before the analysis. Two experiments were carried out for every 250 mL of the water sample:

- (1) as is, without addition of heavy metals;
- (2) with addition of a standard solution containing 10.0 mg/L of Cu(II), Cd(II), Pb(II), Mn(II), and Cr(III) ions.

Briefly, 50 mg of the adsorbent was added to 250 mL of each water sample of the aqueous solution; the pH of the suspensions was adjusted to 7.2–7.8 and it was stirred for 12 h. The solid phase was filtrated and the metal content was determined in the supernatant solution by the inductively coupled plasma optical emission spectrometry (ICP-OES) method.

### 3. RESULTS AND DISCUSSION

**3.1. Adsorbents' Synthesis Strategy.** One-step syntheses with sodium metasilicate or TEOS as the precursor were used for producing SBA-15-type adsorbents. Pluronic P123 as the structure-directing agent (template) was used in both cases. The

surfactant formed rod-like micelles in aqueous medium, on the surface of which joint hydrolytic polycondensation of silica precursors and functional silanes occurred. The general approaches to the mesoporous materials preparation are presented in Scheme 1.

Thus, the obtained adsorbents had a different nature and environment of N-containing functional groups and therefore potentially varied mechanisms of extraction of the investigated heavy metals in cation or anion forms, combined with high kinetic characteristics of the mesoporous silica matrix.

**3.2. Structure Ordering and Characterization of Mesoporous Silica.** All synthesized samples were white, powdered and fine-dispersed. From SEM images, characteristic rod-like morphology of SBA-15 type materials could clearly be seen (Figure S1). The influence of the synthesis conditions on the structural parameters of the obtained samples was investigated using X-ray diffraction analysis (XRD) (Figure 1).

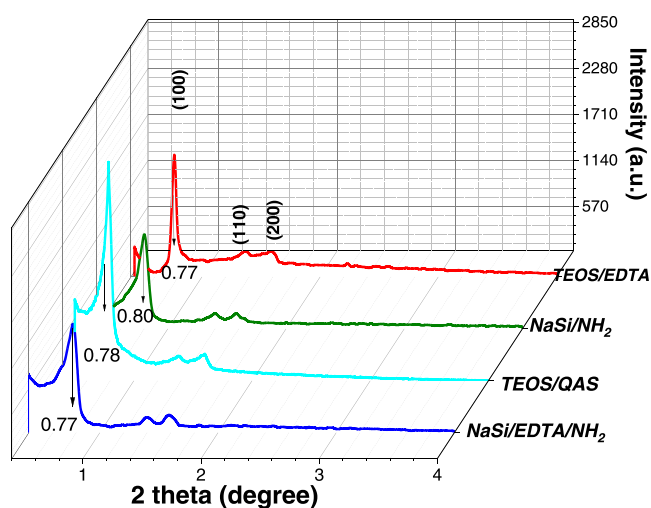


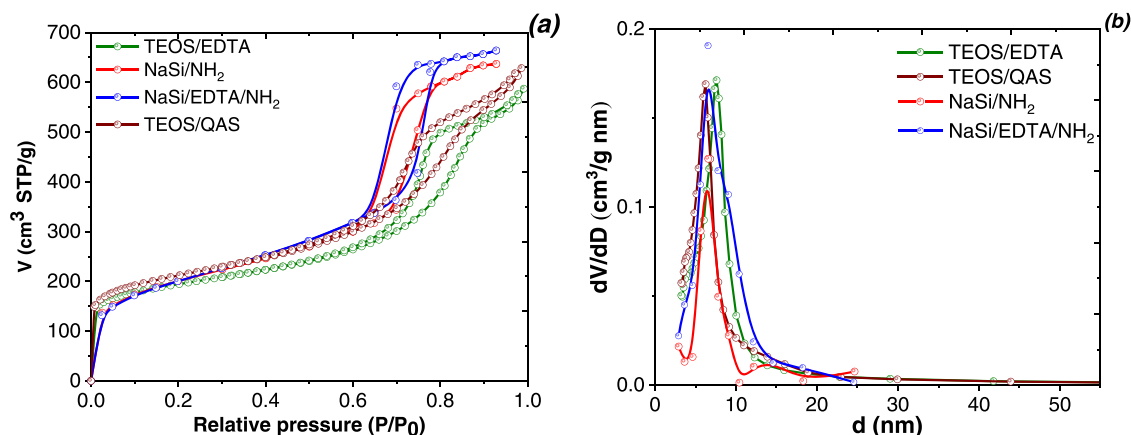
**Figure 1.** Small-angle X-ray scattering patterns for the obtained samples.

The SAXS patterns of all samples show three well-resolved diffraction peaks (see Figure 1). The high intense reflection centered around  $2\theta = 0.8$ , and two low-intensity peaks were observed, which could be indexed to the (100), (110), and (200) planes. These diffraction peaks were characteristic of the formation of a high-degree well-ordered hexagonal  $P6/mmm$

space group. The SBA-15 samples obtained from both silica sources were highly ordered. The relative intensity of the peaks in NaSiO<sub>3</sub>-based adsorbents was somewhat less compared to those synthesized from TEOS.

The N<sub>2</sub> adsorption/desorption data for the prepared samples revealed type IV curves, with a well-defined capillary condensation step and obvious H1 hysteresis loops in the partial pressure range of 0.60–0.85 characteristic of mesoporous materials according to the IUPAC classification (Figure 2).<sup>20</sup> The presence of a hysteresis loop indicated that the structure was two-dimensional (2D) centred. In the case of NaSi/NH<sub>2</sub> and NaSi/EDTA/NH<sub>2</sub>, the capillary condensation occurred at a lower  $p/p_0$  than that for TEOS/EDTA and TEOS/QAS samples. This effect indicated that the structural arrangement was affected by the synthesis route (Scheme 1). The textural properties of the modified SBA-15 materials are summarized in Table 1. High specific surface area values were obtained for all obtained materials. While similar values were exhibited by TEOS/EDTA and TEOS/QAS, for NaSi/NH<sub>2</sub> the represented value was slightly lower. This effect can be explained by the different thicknesses of the mesopore walls of the obtained materials. The specific surface areas of the samples did not decrease with increase in the concentration of functional groups. The average pore sizes varied from 6.6 nm to 7.4 nm (Table 1). Thus, the synthesized materials could be considered mesoporous.<sup>41,42</sup>

All obtained samples had a well-ordered centered rectangular hexagonal structure according to the TEM data (Figure 3). A channel-like ordered structure running parallel to the longer direction similar to the SBA-15-type material of Zhou's<sup>20</sup> and Ryo's<sup>28</sup> reports was observed. The nature of the silica source and ratio of reagents in the reaction mixture, as well as the size of the functionalizing groups, had insignificant effects on the structure formation process. Hence, it was possible to obtain ordered SBA-15-type materials with both applied silica sources and various functional groups. The average thicknesses of the mesopore walls ( $t_w$ ) of TEOS/EDTA, TEOS/QAS, NaSi/NH<sub>2</sub>, and NaSi/EDTA/NH<sub>2</sub> were 60.0, 60.1, 64.3, and 67.7 Å, respectively. The sample prepared from metasilicate exhibited thicker pore walls, which was of great importance for chemical and thermal stability. Thus, the synthesis approaches proposed in these work to obtain functionalized SBA-15 resulted in materials exhibiting similar high mesoporosity and offering potentially good adsorptive features.

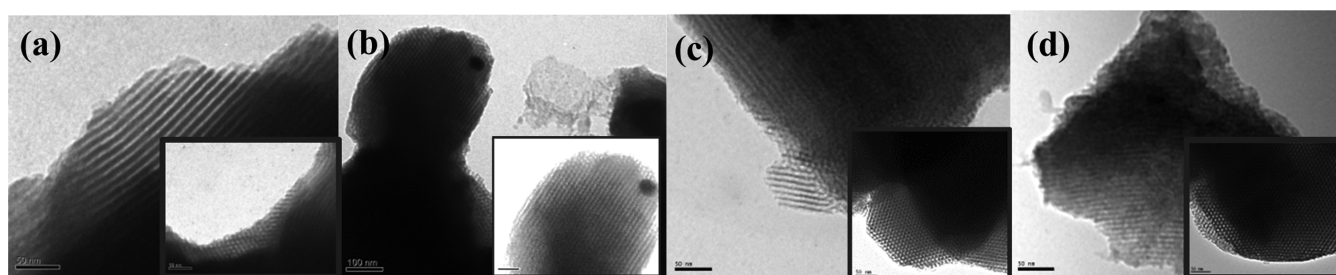


**Figure 2.** N<sub>2</sub> adsorption/desorption isotherms (a) and pore size distributions (b) of the synthesized mesoporous samples.

Table 1. Textural and Quantitative Parameters of Mesoporous Samples<sup>a</sup>

sample	N <sub>2</sub> ad/desorption isotherms			N (%)	elemental analysis			pH-metric titration	
	S <sub>BET</sub> (m <sup>2</sup> /g)	V <sub>total</sub> (cm <sup>3</sup> /g)	d (nm)		C (%)	H (%)	C <sub>L</sub> (mmol/g)	direct	back
TEOS/EDTA	745	1.44	7.4					1.00	
NaSi/NH <sub>2</sub>	700	0.99	6.6	1.74	9.01	3.05	1.26	0.14	0.98
NaSi/EDTA/NH <sub>2</sub>	710	1.03	6.6	1.06	8.57	2.83	0.51/0.25	0.33/0.46	0.60/0.1
TEOS/QAS	730	1.12	7.0	0.92	9.53	3.1	0.82		

<sup>a</sup>S<sub>BET</sub> – Surface area calculated by the BET method; V<sub>total</sub> – volume of adsorbed N<sub>2</sub> at p/p<sub>0</sub> = 0.93; d – pore diameters calculated by BJH; C<sub>L</sub> – concentration of functional groups.

Figure 3. TEM images of N-containing SBA-15 samples: (a) NaSi/NH<sub>2</sub>; (b) NaSi/EDTA/NH<sub>2</sub>; (c) TEOS/EDTA; and (d) TEOS/QAS.

To confirm the success of the synthesis process, samples have been characterized by FTIR (Figure 4). The vibration bands at

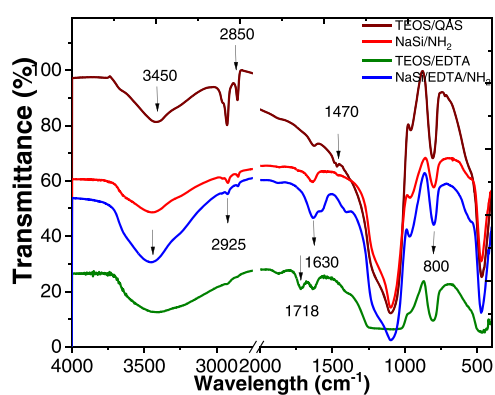


Figure 4. FTIR spectra of the synthesized mesoporous samples.

around 1250, 1080, 800, and 457 cm<sup>-1</sup> present in all obtained samples are typical for Si–O–Si bonds attributed to the condensed silica network. The absorption wide band that appeared at around 3450 cm<sup>-1</sup> was assigned to ν(O–H) stretching. The absorbance peaks corresponding to the ν(C–H) stretching vibrations appeared at 2925 and 2850 cm<sup>-1</sup>; these peaks became intense in all modified materials, the strongest bands being observed for the TEOS/QAS sample. The band around 1470 cm<sup>-1</sup> was assigned to the δ(C–H) bending of the alkyl group. The absorption band at 1600 cm<sup>-1</sup> was assigned to the δ(N–H) bending vibration, confirming the incorporation of NH<sub>2</sub>-groups. The absorbance of the C–N stretching vibration is normally observed around 1000–1200 cm<sup>-1</sup>. As for the NaSi/NH<sub>2</sub> and NaSi/EDTA/NH<sub>2</sub> samples, the weak band at 3300 cm<sup>-1</sup> ascribed to the ν(N–H) of the NH<sub>2</sub>-groups' stretching vibration appeared and was attributed to the stretching vibration of the protonated –NH<sub>3</sub><sup>+</sup> groups. Also, two strong bands at 1630 and 1578 cm<sup>-1</sup> of the NaSi/EDTA/NH<sub>2</sub> sample were

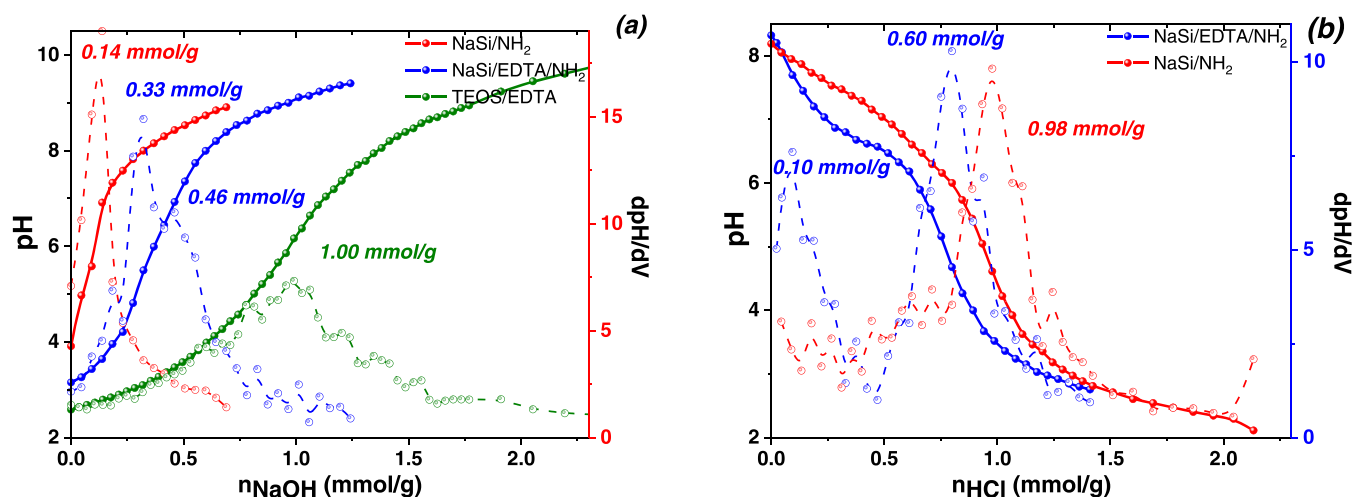
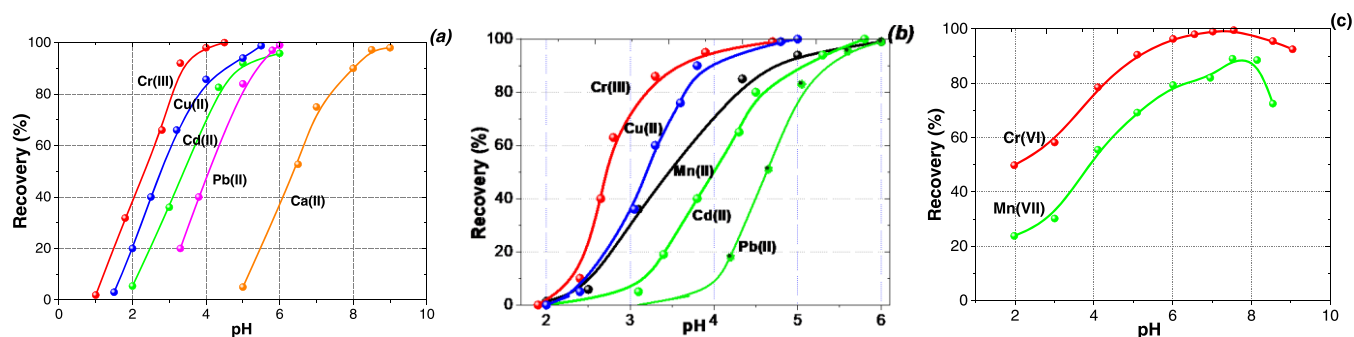


Figure 5. Direct (a) and back (b) pH-metric titration curves with the corresponding 1st derivative for the mesoporous silicas.



**Figure 6.** Effect of pH on the recovery of metal ions by TEOS/EDTA (a), NaSi/EDTA/NH<sub>2</sub> (b), and TEOS/QAS (c) samples (conditions:  $C_M = 2.5 \times 10^{-5}$  mol/L, volume 20 mL, adsorbent dose 0.05 g,  $t =$  overnight).

**Table 2.** Values of the  $pH_{50}$  of Metal Ions on the Obtained Adsorbents

sample	Pb(II)	Cr(III)	Cu(II)	Cd(II)	Cr(IV)	Mn(VII)	Mn(II)
TEOS/EDTA	4.2	2.7	3.2	4.2	-	-	3.4
NaSi/EDTA/NH <sub>2</sub>	5.0	2.9	3.5	4.6	-	-	3.5
NaSi/NH <sub>2</sub>	5.1	3.4	3.2	4.6	-	-	5.1
TEOS/QAS	-	-	-	-	2.5	4.0	-

assigned to the C–O stretching (the –OH bending vibration of water was not considered) and N–H bending vibrations of protonated N-containing groups in EDTA and NH<sub>2</sub>-motives, respectively. The  $\nu_{as}(C=O)$  bands for the TEOS/EDTA sample were observed at 1720 cm<sup>-1</sup>. This value was characteristic of free carbonyls not involved in hydrogen bonding. Similar observations were made for the other materials.

The total amount of functional groups of mesoporous solids was measured by elemental analysis (Table 1). Also, direct and back acid–base potentiometric titrations have been generally used to determine the amounts of protolytic-active groups.<sup>37</sup> The titration curves and corresponding 1st derivative of the samples are represented in Figure 5.

From the amounts of titrant (NaOH or HCl) spent in each sample, the concentration of the specific functional groups on the mesoporous solid surfaces were determined and are summarized in Table 1. The content of the functional groups for the SBA-15 samples determined by elemental analysis and pH-metric titration assays showed different values for some samples. According to Table 1, less amino groups were found in the NaSi/NH<sub>2</sub> sample by direct titration (Figure 5a). This can be attributed to the protonation of the NH<sub>2</sub>-groups through the silanol groups or HCl in the reaction mixture. To solve this problem, a back-titration procedure was tested: an excess of NaOH (pH 8.4) was added during the preparation of the sample suspension. In contrast to the direct titration of NaSi/NH<sub>2</sub>, it showed 0.98 mmol/g functional groups. Two types of functional groups for the NaSi/EDTA/NH<sub>2</sub> sample were observed, with the concentrations of NH<sub>2</sub> and carboxylic groups corresponding to 0.10 and 0.60 mmol/g, respectively (Figure 5b). The TEOS-based approach showed a higher total content of functional groups than the metasilicate-based one.

Finally, we would like to comment on the main difference in formation of the hexagonal structures of SBA-15 from the different synthesis routes. The use of TEOS as silica source confined the synthesis of SBA-15 to a thin sheet, making perpendicular orientation of pores possible. Also, the unique porous structure of SBA-15 was not compromised by the high concentrations of functional groups in the channels. On the other hand, the strong segregation of Pluronic 123 and

metasilicate as the precursor enabled the formation of a well-developed and rigid mesostructure too, keeping the good performance and quality of SBA-15 owing to high specific surface area with good porous structure, which satisfied the requirements for an excellent adsorbent. The minor difference between these mesoporous materials was the lower content of functional groups for the latter. Thus, using sodium metasilicate as the precursor for synthesis of SBA-15 would render mesoporous silicas more economically sustainable.

**3.3. Uptake Behavior of Mesoporous Adsorbents.** The adsorption performance of adsorbents prepared using sodium metasilicate or TEOS as the precursor for synthesis of SBA-15 towards heavy metal ions in aqueous solution was compared. The effect of pH, concentration, interference of macro-components in environmental waters, and other main factors in the adsorption of metal ions on the obtained adsorbents was studied. The regeneration conditions of the adsorbents were also investigated.

**3.3.1. Effect of pH.** Generally, the pH value plays a crucial role in the uptake features of the adsorbents.<sup>15,39</sup> Figure 6 represents the pH effect on the adsorption of cationic and anionic forms of metal ions on mesoporous silicas.

The ion removal capacity by TEOS/EDTA and NaSi/EDTA/NH<sub>2</sub> samples increased with the increase in pH value, and quantitative metal uptake was observed at pH 4–6 for all of the cations studied (Figure 6a,b). The quantitative uptake of cations by the NaSi/EDTA/NH<sub>2</sub> sample was observed at a higher pH than by TEOS/EDTA. This displacement was quite rational because the weakly basic primary amino groups of NaSi/EDTA/NH<sub>2</sub> were partially protonated at lower pH or through intramolecular interactions (zwitterionic form).<sup>43</sup> This influenced considerably the complexing ability of EDTA groups with metal ions and resulted in transformation of the metal-complex formation during the metal ion adsorption.

The order of metal ion adsorption on each adsorbent was generally consistent with the stability constants of the complexes with the functional groups in the silica matrix, i.e., EDTA and NH<sub>2</sub> groups<sup>44</sup> in our case. The affinity of complexing metal ions to the adsorbent is described through the pH value of 50% adsorption ( $pH_{50}$ ). A smaller value of  $pH_{50}$  corresponds to the

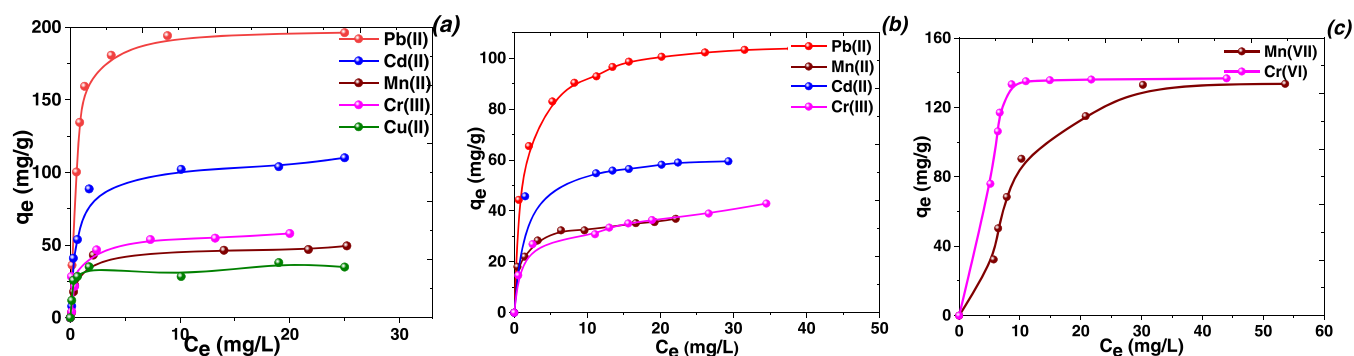


**Figure 7.** Adsorption isotherms of metal ions on TEOS/EDTA (a), NaSi/EDTA/NH<sub>2</sub> (b), and TEOS/QAS (c) samples (conditions: Cd(II) (pH 5.8), Cu(II) (pH 4.0), Pb(II) (pH 6.0), Cr(III) (pH 4.3), Mn(II) (pH 5.5), Mn(VII) (pH 7.5), and Cr(VI) (pH 7.0), adsorbent dose: 0.05 g, volume: 25 mL).

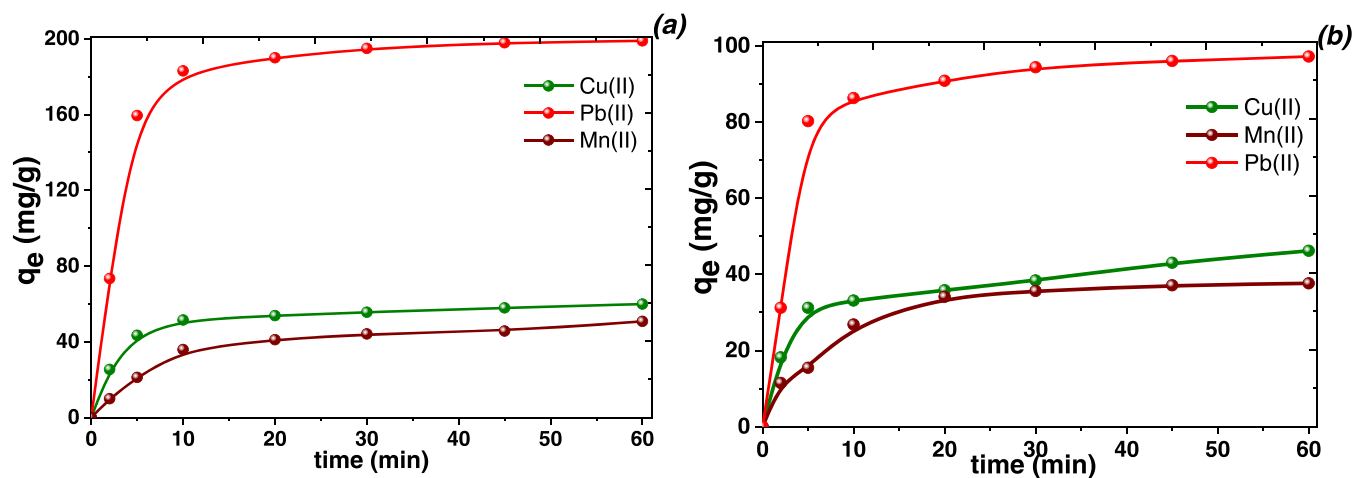


**Figure 8.** Effect of contact time on the removal of Cu(II), Mn(II), and Pb(II) ions by the obtained TEOS/EDTA (a) and NaSi/EDTA/NH<sub>2</sub> (b) samples (conditions:  $C_M$  0.1 mmol/L, adsorbent dose 0.05 mg, volume 25 mL, Cu(II) (pH 4.0), Pb(II), and Mn(II) (pH 6.0)).

formation of more stable metal complexes in the sorbent phase.<sup>45</sup> The type of adsorbent during the uptake process influenced considerably the  $pH_{50}$  value (Table 2). It could be seen that the adsorption affinity of all adsorbents increases significantly with growth of pH.

As can be seen from Table 2, the complexing properties of the NaSi/EDTA/NH<sub>2</sub> sorbent with respect to some transition metals differed from the properties of the monofunctional adsorbents (NaSi/NH<sub>2</sub> and TEOS/EDTA). For example, for Cr(III) and Cd(II) ions, the  $pH_{50}$  values were significantly lower, which indicated a greater strength of their complexes formed on the surface of NaSi/EDTA/NH<sub>2</sub>.

The highest removal percentage of anionic metal forms (CrO<sub>4</sub><sup>2-</sup> and MnO<sub>4</sub><sup>-</sup>) on the anion exchanger (TEOS/QAS) was observed in the pH range from 5 to 8 (Figure 6c), and reached quantitative extraction for Cr(VI). However, Mn(VII) ion uptake on the same adsorbent was not quantitative. This fact could be explained in the following ways: (a) dissociation of silanol groups on the adsorbent surface, which already had a negative charge at high pH and interacted with positively charged quaternary ammonium functional groups, leading to a decrease in the ion-exchange properties of the adsorbent; (b) dissolution of silica matrices at high pH. Thus, for removal of CrO<sub>4</sub><sup>2-</sup> and MnO<sub>4</sub><sup>-</sup> with TEOS/QAS, a pH of the solution close to the pH of environmental water (from 7.0 to 8.0) was used as optimum for further studies.

**3.3.2. Adsorption isotherms.** To characterize the interaction of metal ions with the obtained adsorbents, the adsorption isotherms were studied in static conditions (Figure 7).

All of the isotherms showed a sharp initial slope (Henry's region), indicating that TEOS/EDTA, NaSi/EDTA/NH<sub>2</sub>, and TEOS/QAS act as highly efficient adsorbents at low metal concentrations (Figure 7). These isotherms were predominantly L- and H-type in Giles classification<sup>46</sup> and, in fact, represented adsorbents with a high affinity toward the adsorbate. At optimized removal conditions (Figure 6), the TEOS/EDTA adsorbents synthesized using TEOS as the silica source and bearing chelating groups exhibited the highest maximum adsorption capacity to heavy ions among all of the materials evaluated (Figure 7): 49.4 mg/g (0.90 mmol/g) for Mn(II), 58.7 mg/g (0.92 mmol/g) for Cu(II), 111.2 mg/g (0.98 mmol/g) for Cd(II), 57.6 mg/g (1.01 mmol/g) for Cr(III), and 195.6 mg/g (0.94 mmol/g) for Pb(II). The NaSi/EDTA/NH<sub>2</sub> solids had a relatively high affinity for heavy metal ions according to the shapes of the isotherms too. The observed different affinities in interaction with TEOS/EDTA and NaSi/EDTA/NH<sub>2</sub> samples for each of the heavy metals led to the conclusion that the improvement in attraction should be attributed to the simultaneous presence of NH<sub>2</sub> and EDTA groups.

The adsorption affinity of the EDTA-functionalized samples (NaSi/EDTA/NH<sub>2</sub> and TEOS/EDTA) followed the order Pb(II) > Cd(II) > Cu(II) > Cr(III) > Mn(II). These results could be explained for TEOS/EDTA based on the Pearson

theory of “Hard and Soft Acids and Bases”.<sup>47</sup> According to this theory, the EDTA and NH<sub>2</sub> functional groups are considered as hard base ligands with a high ability to bind to a hard acid. In our case, the Cr(III) and Mn(II) ions with multiple charges and small radii were such hard acids. Other *d*-metal ions (Cu(II), Cd(II), and Pb(II)) were taken as intermediate cases capable of binding to both hard and soft bases. Their polarization was expected to play an important role in the interaction between the metal ions and functional groups when they were having the same charge. The larger the metal ion radius is, the greater the polarization would be. So, the sequence of bonding strength should be Pb(II) > Cd(II) > Cu(II) > Cr(III) > Mn(II). This result did not correlate with the electronegativity of metals for the NH<sub>2</sub>-group-containing silica samples.<sup>25</sup>

**3.3.3. Adsorption Kinetics.** The effect of contact time on the removal of Cu(II), Mn(II), and Pb(II) by TEOS/EDTA and NaSi/EDTA/NH<sub>2</sub> is shown in Figure 8.

The results shown in Figure 8 indicate that Cu(II) and Mn(II) were quantitatively adsorbed by TEOS/EDTA within 10 min, which indicates fast adsorption. However, in the case of Pb(II), the adsorption equilibrium was achieved within 20 min. It has to be noted that the removal of metal ions by NaSi/EDTA/NH<sub>2</sub> followed the order Cu(II) > Mn(II) > Pb(II). But overall, the adsorption efficiencies of the three studied metal ions were over 90.0% after 10 min. At the beginning, adsorption was fast due to the complexation between the metal ions and the available active sites of the mesoporous adsorbents. Similar results have been reported for the removal of heavy metals on functionalized mesoporous adsorbents by Da’na et al.<sup>48</sup> At the same time, the kinetic parameters for the obtained samples were significantly better than those for the EDTA-functionalized silica gel-based adsorbents.<sup>49</sup>

The change in concentration of target metal ions in the adsorption process can be used to fit the adsorption kinetics. The adsorption kinetics of metal ions on the obtained mesoporous adsorbents was estimated using the pseudo-first-order<sup>50</sup> and pseudo-second-order<sup>51</sup> equations, and the calculated data are presented in Table S1. The values of regression coefficient obtained by the pseudo-second order model are much higher than those obtained by the pseudo-first-order kinetic model for Cu(II), Mn(II), and Pb(II), revealing that the adsorption of all three metals followed pseudo-second-order kinetics. Furthermore, the calculated values of  $q_e$  are close to the experimental  $q_e$  values for pseudo-second-order kinetics, indicating that pseudo-second-order model fitted well the experimental adsorption data for Cu(II), Mn(II), and Pb(II) ions. Since these kinetics models do not give information about the diffusion type of target ions on the adsorbents, the Weber-Morris (intraparticle diffusion) model<sup>52</sup> was used to determine the diffusion mechanisms of Cu(II), Mn(II), and Pb(II) into the porous structure of the samples. It can be seen (Figure S3) that two curves were used for fitting the kinetic data. The first linear part represents the external surface adsorption (film diffusion) and is shown as a fast process, while the second linear part described the intraparticle diffusion as a slow process. These results revealed that both film diffusion and intraparticle diffusion were involved in the adsorption of the studied heavy metal ions onto the obtained adsorbents.

**3.3.4. Selectivity Test.** In order to examine the selectivity of the adsorbents, competitive sorption of metal ions from their multicomponents mixtures was investigated in batch experiments. Also, the effect of different common inorganic ions, which can occur in environmental samples, was crucial when

evaluating the adsorbents for water treatment applications. The selectivity factor of the adsorbents was reflected by the  $K_d$  value (Figure 9).

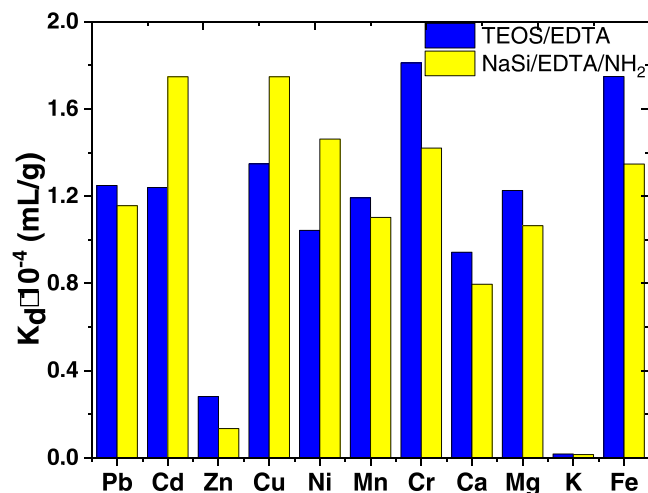


**Figure 9.** Metal ion adsorption in multicomponent solutions on TEOS/EDTA and NaSi/EDTA/NH<sub>2</sub> samples (conditions: C(M) = 5 mg/L, time 30 min, adsorbent dose 50 mg, volume 50 mL, pH 6.0).

The TEOS/EDTA sample had a higher removal ability for Cd(II), Pb(II), and Cu(II) over Na(I), K(I), and Zn(II) ions, as shown in Figure 9. A higher separation factor implying higher removal of target heavy metal ions (Cd(II), Cu(II), Pb(II), and Cr(III)) was obtained with even as little as 50 mg of TEOS/EDTA. The affinity of the NaSi/EDTA/NH<sub>2</sub> sample was consistent with the following selectivity order: Pb(II) ≥ Cu(II) ~ Cd(II) ≫ Ni(II) > Cr(III). The high selectivity for Pb(II), Cu(II), and Cd(II) by NaSi/EDTA/NH<sub>2</sub> could be due to the higher complexing constant of the formed heteroatomic complex of these metal ions, which facilitates their transport to the mesoporous material’s surface, thus favoring their preferential removal by the obtained adsorbents.

**3.3.5. Effect of Coexisting Ions.** Real aqueous systems contain a lot of inorganic ions (Table 3), which can significantly influence the adsorbent’s efficiency towards target heavy metals. Knowledge of the impact of the main ions present in environmental samples on the uptake of pollutants is crucial when evaluating the adsorbent’s application for water treatment. The interference effects caused by the presence of cations and anions in the matrix, among them K<sup>+</sup>, Na<sup>+</sup>, Ca<sup>2+</sup>, Mg<sup>2+</sup>, Al<sup>3+</sup>, Fe<sup>3+</sup>, Zn<sup>2+</sup> (from their nitrate salts) and HPO<sub>4</sub><sup>2-</sup>, SO<sub>4</sub><sup>2-</sup>, CO<sub>3</sub><sup>2-</sup>, Cl<sup>-</sup> (from their sodium salts) ions, respectively, on the removal of representative heavy metals was investigated (Table 3). Adsorptive experiments under the optimum conditions described above for adsorption from model solutions were performed. The initial concentration of all metal ions in solution was 1 mg/L.

The K<sup>+</sup> ions exerted almost no suppressive effect on the adsorption of heavy metals. The uptake of Cr(III) and Pb(II) ions remained high in the presence of excess quantities of the interfering species. The Fe(III) and Mg(II) ions, which formed highly stable complexes with EDTA in solution, had no considerable effect on the removal of heavy ions by the obtained adsorbents. The recovery of chromate ions by the TEOS/QAS sample practically did not change in the presence of divalent anions. The uptake of CrO<sub>4</sub><sup>2-</sup> by the protonated NaSi/EDTA/

**Table 3. Effect of Coexisting Ions on the Recoveries of the Determined Metal Ions by Various Adsorbents (pH = 7.0–7.2,  $n = 5$ )**

ions	C, mg/L	recovery (%)					
		TEOS/EDTA		NaSi/EDTA/NH <sub>2</sub>		TEOS/QAS	
		Pb(II)	Cr(III)	Pb(II)	Cr(III)	CrO <sub>4</sub> <sup>2-</sup>	CrO <sub>4</sub> <sup>2-</sup>
K(I)	12 000	101 ± 1.3	101 ± 1.9	104 ± 0.8	106 ± 0.3	101 ± 1.3	101 ± 1.9
Na(I)	1000	95 ± 0.9	98 ± 1.4	99 ± 1.5	98 ± 0.4	95 ± 0.9	99 ± 1.3
Ca(II)	5000	95 ± 0.8	92 ± 0.9	96 ± 1.3	99 ± 0.5	95 ± 0.8	102 ± 0.5
Mg(II)	100	84 ± 1.4	90 ± 0.7	94 ± 0.6	87 ± 1.7	84 ± 1.4	101 ± 0.2
Zn(II)	100	84 ± 1.4	90 ± 0.7	94 ± 0.6	87 ± 1.7	84 ± 1.4	100 ± 0.7
Co(II), Ni(II)	10	82 ± 1.1	89 ± 0.6	93 ± 0.7	85 ± 1.4	82 ± 1.1	99 ± 0.9
Cl <sup>-</sup>	5000	99 ± 0.9	101 ± 1.4	102 ± 1.5	101 ± 0.4	99 ± 0.9	101 ± 1.4
Br <sup>-</sup>	100	96 ± 0.7	96 ± 0.7	97 ± 1.4	99 ± 0.8	96 ± 0.7	91 ± 0.7
SO <sub>4</sub> <sup>2-</sup>	5000	95 ± 0.8	92 ± 0.9	98 ± 1.3	99 ± 0.5	95 ± 0.8	92 ± 0.9
HPO <sub>4</sub> <sup>2-</sup>	5000	99 ± 1.4	98 ± 0.7	99 ± 0.6	97 ± 1.6	70 ± 1.4	91 ± 0.6
NO <sub>3</sub> <sup>-</sup>	5000	95 ± 0.9	98 ± 1.4	99 ± 1.5	98 ± 0.7	75 ± 0.9	95 ± 1.0
humic acid	70	99 ± 0.8	97 ± 0.9	98 ± 1.0	96 ± 0.6	99 ± 0.9	96 ± 1.0
fulvic acid	50	95 ± 0.8	95 ± 0.6	97 ± 1.6	97 ± 0.8	95 ± 0.8	95 ± 0.9

NH<sub>2</sub> sample was significantly affected by the main inorganic anions (SO<sub>4</sub><sup>2-</sup>, CO<sub>3</sub><sup>2-</sup>, Cl<sup>-</sup>). The recovery of CrO<sub>4</sub><sup>2-</sup> ions by NaSi/EDTA/NH<sub>2</sub> decreased from 99 to 70%. This demonstrated that the obtained adsorbents had good tolerance to the main coexisting ions in environmental water. Thus, the adsorbents were suitable for environmental remediation from heavy metals.

**3.3.6. Desorption Studies.** The reusability possibility of an adsorbent is an important parameter considered to evaluate its economic prospects for practical application. Also, these studies can help in understanding the mechanism of adsorption of the metal ions. The choice of the suitable eluent is important for the practical performance of the developed water treatment procedure in future. Under strong acidic conditions, the coordination interaction of metal ions can be easily disrupted and they can subsequently be released into the desorption medium. The attempts to eluate metal ions were made using HCl, HNO<sub>3</sub>, and EDTA solutions, respectively, exploiting either protonation of ligands or competition in complexation (Table S2, Supporting information). It was found that desorption of cations increased with increasing acid concentration. This was apparently due to increased protonation of the N-containing sites on silica. The more efficient elution by 0.5 mol/L HNO<sub>3</sub> (recovery 99%) in comparison to 1 mol/L HCl (recovery 92.0%) was observed due to its stronger complexing ability with metal ions. Challenges in the desorption of metal ions from the surface of adsorbents could be caused by the much stronger binding to functional groups in the inner-sphere complexes, resulting in difficulty in removing the metal ions from the adsorbent surface just by changing the pH of the solution.

To determine the optimal conditions for selective elution from metal-loading adsorbents, a series of experiments were performed in the dynamic desorption conditions (“gradient elution”) with diluted HNO<sub>3</sub> (Figure 10).

The efficiencies of desorption for all of the metal ions on the poly-functionalized adsorbent ranged between 38 and 85% (Figure 10). It was obvious that when the rate of the acidic elution decreased or the concentration of eluent increased, the recovery of all metal ions increased significantly. These data confirmed the possibility of selective desorption of the required ions during the analysis of various objects (mineral waters, wastewater, artesian water, biological fluids, etc.). For example, the Cd(II) or Cr(III) ions could be eluted by a solution of nitric acid with pH = 2.5–4.0 in the presence of the Fe(III) and Cu(II)

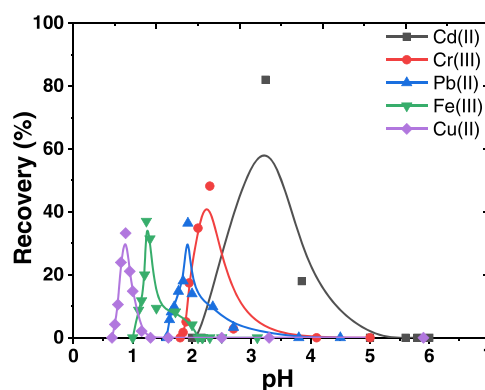


**Figure 10.** Effect of pH on the elution of metal ions from the NaSi/EDTA/NH<sub>2</sub> sample (conditions: weight 1.0 g, rate of solution 1 mL/min, C(HNO<sub>3</sub>) = 0.05 mol/L).

ions, which could be present in large quantities in the analyzed natural and wastewater matrices and thus interfere with the selective determinations.

**3.3.7. Regeneration Studies.** A satisfactory eluent should effectively eluate the adsorbed heavy metals by not altering the adsorptive performance of adsorbents. The textural and quantitative parameters of the mesoporous samples were investigated before and after the desorption experiments (Figure 11).

The amount of functional groups on the surface of the series of mesoporous samples only slightly decreased (~1–5%) after the first regeneration cycle (Figure 11). Moreover, after desorption on the NaSi/EDTA/NH<sub>2</sub> sample, it was used again with nearly the same parameters as the silica matrix (Table 1). The essential decrease in adsorption amount by the TEOS/EDTA and TEOS/QAS samples was supposedly due to the formation of “arched” structures of functional groups, partially blocking the entrance to the mesoporous channels.<sup>15</sup> Especially, this effect is typical for huge functional groups on the surface. As can be seen from Figure 11, the surface area of both the SBA-15 matrices is not decreased after the first regeneration cycle.

Figure 12 depicts the value of the specific surface area after four consecutive adsorption/desorption cycles of TEOS/EDTA and NaSi/EDTA/NH<sub>2</sub> samples. As we can see, after each consecutive cycle, the surface area of the sample decreases and reaches a value of 256 m<sup>2</sup>/g<sup>1</sup> after four cycles, which is about

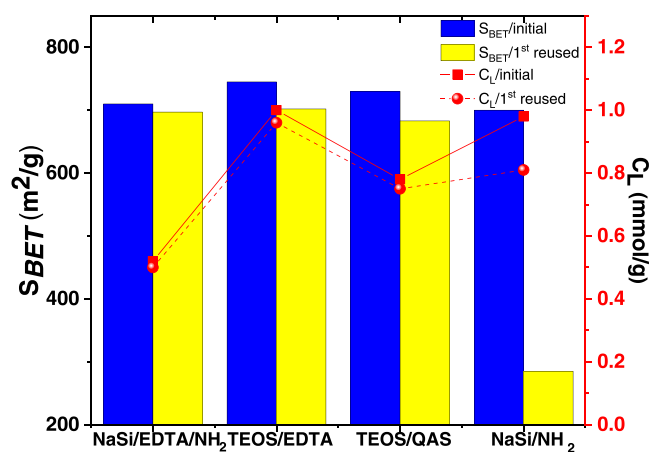
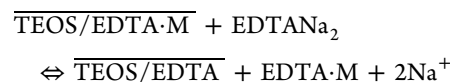


**Figure 11.** Comparative textural and quantitative parameters of the mesoporous adsorbents after the first regeneration cycle using HNO<sub>3</sub> (0.05 M).

36.1% of the surface area of the initial NaSi/EDTA/NH<sub>2</sub> sample. The pH-metric titration of the regenerated NaSi/EDTA/NH<sub>2</sub> after four consecutive cycles was carried out to check the loss of EDTA and NH<sub>2</sub> groups. It confirmed around 19.1% loss (or blocked in the pores) of functional groups from the NaSi/EDTA/NH<sub>2</sub> sample, but this loss was not significant enough to explain the 19% loss of functional groups on the SBA-15 sample by four consecutive cycles. Therefore, the decrease might be due to the loss of functionality from the adsorbent as well as the partial blocking of the binding sites of EDTA and NH<sub>2</sub> groups by the adsorbed (undesorbed) metal ions.

Also, SBA-15-based adsorbents functionalized with chelating groups (TEOS/EDTA and NaSi/EDTA/NH<sub>2</sub>) after metal ion adsorption can be regenerated by a solution of strong acids or competing chelating eluents (Table S2). Ethylenediaminetetraacetic acid and other aminopolycarboxylic derivatives in solution are known to form stable chelates with metal ions.<sup>33</sup> Thus, the metal ions adsorbed on the adsorbents could be removed from the adsorbents as a result of the complexation reaction with the EDTA disodium salt solution



To shift the equilibrium to the right, the eluent must form more stable complexes with heavy metal ions than with functional groups on the surface, or use an excess of eluent.

Various concentrations of EDTA disodium salt solution have been tested for regeneration of metal-loaded mesoporous samples (Table S2). It is clear that the performance of the EDTA disodium salt for the regeneration of adsorbents was higher with increased concentrations up to 1 M.

The regeneration of selected adsorbents using the EDTA disodium salt as desorption agent is presented in Figure 13.

The uptake capacity did not change in five to six regeneration cycles when using chelating agent treatment (Figure 13). Under such conditions, the adsorbed cations were completely removed from the adsorbent surface, the process, however, being much slower compared to acid treatment. The obtained effect showed that the complexes of metal ions on the surface were considerably less stable than the complexes in solution. This effect is a known phenomenon for adsorbents, which contain functional groups covalently bonded with the surface.<sup>37</sup>

Overall, the experimental data showed that these materials have reasonably good recycling and regeneration abilities.

**3.4. Application of adsorbents for the remediation of environmental water samples.** The obtained adsorbents were applied to the environmental remediation of contaminated water samples from heavy metal ions (Cd(II), Cu(II), Pb(II), Mn(II, VII), and Cr(III, VI)). The initial pH and other parameters of natural water samples tested during 1 year are summarized in Table 4.

This information can guide the prioritization of environmental areas requiring remediation. The MRL values of heavy metal ions in drinking water according to WHO guidelines<sup>53</sup> were 0.003, 1.50, 0.05, 0.39, and 0.05 mg/L for Cd(II), Cu(II), Pb(II), Mn(II), and Cr(III), respectively. As demonstrated in Table 4, three heavy metal ions were detected in the lake and river water, with concentrations higher than the environmental quality standards.<sup>53</sup> This may be attributed to the industrial and anthropogenic activities along the side of the environmental water in the urban city.<sup>54</sup> The highest concentration of Mn(II) was registered at 18.41 μg/L (river water). Generally, the mean

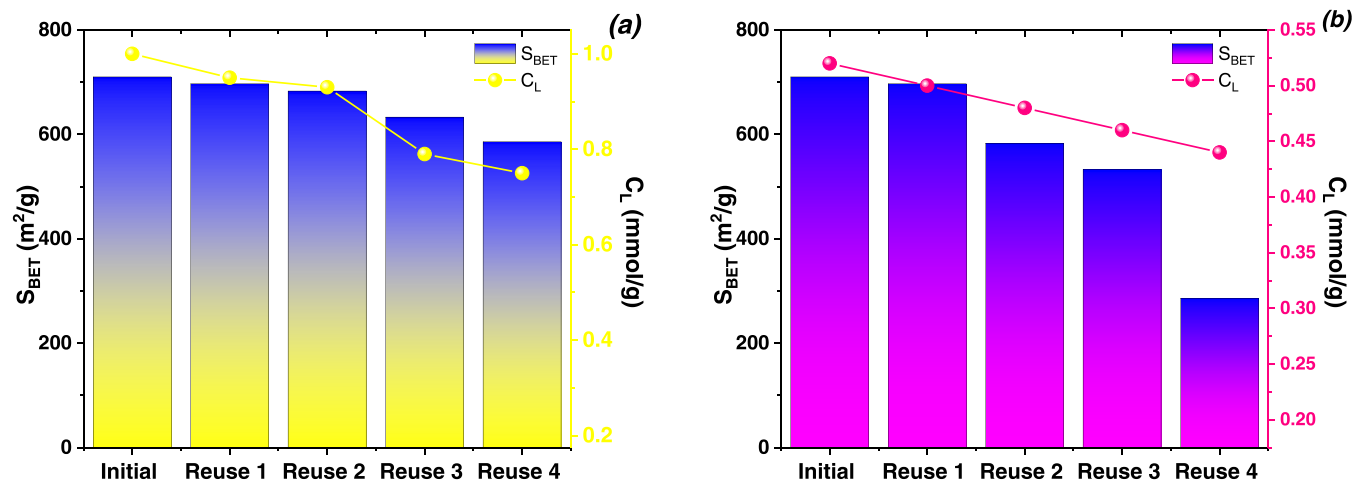


**Figure 12.** Regeneration performance of TEOS/EDTA (a) and NaSi/EDTA/NH<sub>2</sub> (b) samples (conditions: pH 1.0 (by HNO<sub>3</sub>), volume of eluate 2.0 mL, adsorbent dose 50 mg, time contact 2 h).

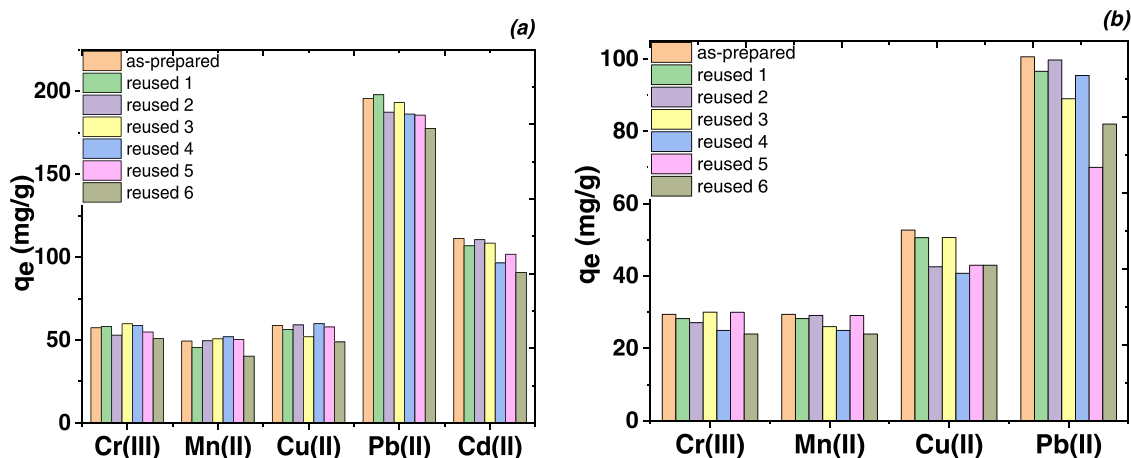


**Figure 13.** Reusability of TEOS/EDTA (a) and NaSi/EDTA/NH<sub>2</sub> (b) toward the heavy metal ion removal during consecutive regeneration cycles (conditions: eluent 1 M EDTANa<sub>2</sub>, volume solution 5 mL, contact time 2 h).

**Table 4.** Distribution of the Main Components of Natural Water Samples in Different Seasons of 2020/2021 (Monitoring Data)

parameter	december 2020		june 2021		december 2021	
	Dnipro <sup>a</sup> river water	artesian <sup>b</sup> drinking water	Dnipro river water	artesian drinking water	Dnipro river water	artesian drinking water
General Parametrs						
pH	7.97	7.40	7.67	7.70	7.39	7.52
Dry residue, mg/L	2227	601	1688	531	2278	640
Water hardness total, mg-eqv/L	16.6	8.5	23.6	12.5	18.6	8.5
Alkalinity (total), mg-eqv/L	10.0	8.5	9.0	8.5	9.2	7.6
Main Cations and Anions (Macrocomponents)						
Ca, mg/L	138.5	47.5	208.5	47.5	200.5	39.4
Mg, mg/L	64.4	19.5	70.4	19.5	69.6	19.5
K, mg/L	1.2	1.0	1.1	1.2	1.1	0.9
Na, mg/L	26.4	7.3	80.1	7.0	85.4	7.6
Cl <sup>-</sup> , mg/L	153	43.7	170	41.7	135	44.1
HCO <sub>3</sub> <sup>2-</sup> , mg/L	193	470.7	200	463.7	177	488.1
SO <sub>4</sub> <sup>2-</sup> , mg/L	182.4	126.6	250.4	116.2	341.4	122.4
F <sup>-</sup> , mg/L	0.60	0.30	0.40	0.35	0.49	0.15
Biogenic Elements						
NO <sub>3</sub> <sup>-</sup> , mg/L	43.0	0.5	43.0	0.5	43.0	0.5
NO <sub>2</sub> <sup>-</sup> , mg/L	≤0.015	≤0.02	≤0.015	≤0.02	≤0.015	≤0.02
HPO <sub>4</sub> <sup>2-</sup> , mg/L	0.28	0.05	0.12	0.06	0.19	0.05
Si, mg/L	8.2	7.5	8.5	8.4	13.2	8.0
Microcomponents***						
Fe (total), mg/L	0.014	≤0.02	0.015	0.05	0.09	≤0.02
Mn (total), mg/L	0.013	0.002	0.04	0.003	0.018	0.004
Cu, mg/L	0.001	0.002	0.004	0.003	0.005	0.006
Zn, mg/L	0.06	0.01	0.06	0.01	0.07	0.005
Pb, mg/L	0.001	0.0001	0.001	0.0001	0.002	0.0001
Cd, mg/L	0.001	0.0004	0.0016	0.0002	0.0019	0.0003
Cr(total), mg/L	0.001	0.001	0.001	≤0.003	0.001	≤0.004
Organic Components						
total organic carbon, mg/L	2.5	1.1	13.7	1.0	17.9	1.9

<sup>a</sup>Footbridge (center Kyiv, Ukraine). <sup>b</sup>Taras Shevchenko Park (center Kyiv, Ukraine).

concentration of heavy metals in the surface water of river Dnipro (Ukraine) is in the following order: Mn(total) > Cu(II) > Cr (total) > Cd(II) ~ Pb(II). The concentrations of Pb(II) ranged between 1.0 and 2.0 μg/L in the different seasons of the years. The lowest concentration of Pb(II) (0.01 μg/L) was recorded in the artesian water.

The artesian drinking and several environmental water samples were decontaminated using the obtained mesoporous

adsorbents. The concentrations of metal ions in the tested water samples before and after treatment are summarized in Table 5. All of the collected water samples were analyzed with and without spiking by inorganic pollutants (0 or 10 μg/L).

In general, as demonstrated in Table 5, all of the obtained adsorbents (synthesized using TEOS and Na<sub>2</sub>SiO<sub>3</sub>) showed comparable adsorption properties for heavy metal ions in environmental water. Following adsorption of spiked metal ions

**Table 5. Experimental Data of Heavy Metal Ion (Label Forms) Removal from Real Water Samples by the Obtained Mesoporous Adsorbents<sup>a</sup>**

sample	metal ion	$C^b$ , $\mu\text{g/L}$	added ( $\mu\text{g/L}$ )		found ( $\mu\text{g/L}$ )				
			0	10	TEOS/EDTA	NaSi/EDTA/NH <sub>2</sub>	NaSi/NH <sub>2</sub>	TEOS/QAS	
artesian drinking water	Cd(II)	0.3	0	10	0.01	0.10	0.05	0.3	
			0	10	5.83	5.77	4.18	3.79	
	Cu(II)	6.0	0	10	0.8	0.9	1.8	5.7	
			0	10	2.8	3.7	6.5	9.4	
	Pb(II)	0.1	0	10	0.01	0.05	0.07	0.1	
			0	10	5.56	6.15	5.67	5.5	
	Mn(total)	3.0	0	10	1.8	2.0	2.9	1.2	
			0	10	2.8	3.0	4.9	6.2	
	Cr(total)	4.0	0	10	0.4	1.7	3.4	2.2	
			0	10	2.4	2.9	5.4	7.2	
	river water (Dnipro, Ukraine)	Cd(II)	1.9	0	10	1.33	1.55	0.01	1.85
				0	10	0.33	0.65	3.01	1.93
Cu(II)		5.0	0	10	1.1	1.1	0.61	4.92	
			0	10	1.9	1.1	3.61	8.56	
Pb(II)		2.0	0	10	0.87	0.82	0.98	2.0	
			0	10	1.07	1.82	5.98	11.0	
Mn(total)		13.0	0	10	5.1	6.6	7.9	7.4	
			0	10	10.1	9.5	11.8	16.4	
Cr(total)		1.0	0	10	0.12	0.21	0.08	0.06	
			0	10	1.89	6.21	8.18	4.89	
lake water (Virlytca, Kyiv, Ukraine)		Cd(II)	5.0	0	10	3.43	3.13	3.89	3.48
				0	10	1.11	4.78	6.19	10.76
	Cu(II)	9.0	0	10	2.1	1.3	1.93	8.3	
			0	10	2.34	4.24	5.5	12.8	
	Pb(II)	9.0	0	10	5.67	4.15	5.85	8.15	
			0	10	5.01	9.65	9.15	4.03	
	Mn(total)	18.0	0	10	8.6	7.9	7.9	11.9	
			0	10	2.9	5.78	9.0	10.76	
	Cr(total)	2.0	0	10	0.12	0.11	0.11	1.01	
			0	10	1.89	1.97	5.34	7.74	

<sup>a</sup>The analyzed water volume was 250 mL, pH 7.0–7.5, adsorbent dose 100 mg, time contact 12 h. <sup>b</sup>Determined by the ICP-OES method with the standard procedure.

onto TEOS/EDTA and NaSi/EDTA/NH<sub>2</sub> samples, a removal efficiency of over 96% for all metal ions in the studied spiked water samples was obtained. The loading capacities of adsorbents were between 45–50 mg/g, which was comparable to the concentrations of the functional groups (Table 1) of adsorbents. The incredible removal capacity of TEOS/QAS over other obtained mesoporous adsorbents towards Mn(VII) and Cr(VI) could be due to its strong anion-exchange functional groups (Table 5). Thus, the adsorbents were able to quantitatively adsorb the various concentrations of the cationic and anionic forms of heavy metal ions (for example, Cu(II), Cr(III, VI), etc.) originally present in all of the water types. The high capacity and selectivity provided by TEOS/QAS, TEOS/EDTA, and NaSi/EDTA/NH<sub>2</sub> samples for heavy metal ion removal, far above other engineered adsorbents, make them potential adsorbents for removing heavy metals (especially Cd(II), Cr(III, VI), and Pb(II)) from contaminated environmental waters.<sup>54</sup> The advantage of the obtained materials was their good resistance to the interfering components of the studied water matrix, which suggested that TEOS/QAS, TEOS/EDTA, and NaSi/EDTA/NH<sub>2</sub> samples were promising adsorbents for the heavy metal ions' decontamination under diverse chemical conditions. Thus, the developed strategy is accurate, reliable, and can be used for the environmental

remediation of contaminated water resources by heavy metal ions.

In addition, the cost of the adsorbents obtained by various approaches was evaluated, because it is an important factor for their practical application in water treatment technologies. Evaluation of the cost of adsorbents consisted of the prices of the starting reagents (Table S3) without direct labor, energetic sources, and manufacturing overhead. The estimated price indicated that use of the metasilicate-based method decreases the synthesis cost by around 10% compared to those prepared from TEOS. Since the major part (>50%) of the cost of synthesis of mesoporous adsorbents is commercial functionalized organosilanes, it is noteworthy that the SBA-15-based functionalized samples obtained from TEOS exhibited similar adsorption performance with higher reusability than those prepared from sodium metasilicate, which made both silica sources suitable for the large-scale production of mesoporous adsorbents.

Thereby, this can be considered as a feasible approach for adsorption water treatment from the points of view of ecology and economy for industrial applications.

#### 4. CONCLUSIONS

Mono- and bifunctionalized mesoporous silicas of the SBA-15 family were prepared using two different silica sources, TEOS and sodium metasilicate. The obtained materials were evaluated

as adsorbents for decontamination of environmental water, from both the adsorption efficiency and economical points of view. All synthesized materials exhibited a high surface area (up to 760 m<sup>2</sup>/g) and an average pore diameter in the mesoporous range, and demonstrated proficient removal of toxic heavy metal ions. The products obtained from tetraethoxysilane showed higher adsorption capacities toward heavy metal ions than those obtained from sodium metasilicate. The overall selectivity in the order Cr(III) > Cu(II) > Cd(II) > Pb(II) > Mn(II) and Cu(II) > Cd(II) > Cr(III) > Pb(II) > Mn(II) was observed for TEOS/EDTA and NaSi/EDTA/NH<sub>2</sub> adsorbents, respectively. The selectivity of the TEOS/QAS sample toward Cr(VI) and Mn(VII) ions at high pH indicated its potential for selective removal of metal anions. The desorption study indicated that adsorbents could easily be regenerated using an acidic/basic solution and reused several times without significant loss in their adsorption efficiency. The studied mesoporous adsorbents were efficient for remediation of multielement-contaminated environmental water from toxic metal ions. The matrix effects in such a procedure were reasonably tolerable. Thus, potentially sustainable high-quality SBA-15-type adsorbents were obtained from sodium metasilicate. This procedure was highly reproducible and suitable for the large-scale synthesis of adsorbents for environmental remediation.

## ■ ASSOCIATED CONTENT

### SI Supporting Information

The Supporting Information is available free of charge at <https://pubs.acs.org/doi/10.1021/acsomega.2c02151>.

Electronic supporting information available (Figure S1, S2 and S3; Table S1, S2 and S3): additional data of characterization of adsorbents (SEM data), regeneration conditions, forms of metal ions in solution and cost estimation of mesoporous adsorbents (PDF).

## ■ AUTHOR INFORMATION

### Corresponding Author

Natalia G. Kobylinska – *A.V. Dumansky Institute of Colloid and Water Chemistry, NAS of Ukraine, Kyiv 03680, Ukraine*;  
✉ [orcid.org/0000-0001-8181-1451](https://orcid.org/0000-0001-8181-1451); Email: [kobilinskaya@univ.kiev.ua](mailto:kobilinskaya@univ.kiev.ua)

### Authors

Vadim G. Kessler – *Department of Molecular Sciences, Swedish University of Agricultural Sciences, 75007 Uppsala, Sweden*;  
✉ [orcid.org/0000-0001-7570-2814](https://orcid.org/0000-0001-7570-2814)

Gulaim A. Seisenbaeva – *Department of Molecular Sciences, Swedish University of Agricultural Sciences, 75007 Uppsala, Sweden*; ✉ [orcid.org/0000-0003-0072-6082](https://orcid.org/0000-0003-0072-6082)

Oksana A. Dudarko – *Chuiiko Institute of Surface Chemistry of NAS of Ukraine, Kyiv 03164, Ukraine*

Complete contact information is available at:  
<https://pubs.acs.org/10.1021/acsomega.2c02151>

### Notes

The authors declare no competing financial interest.

## ■ ACKNOWLEDGMENTS

The authors are grateful to the Ministry of Education and Science of Ukraine “Creation of novel organic-inorganic hybrid materials as sorbents for wastewater treatment from heavy metal ions” (2019–2021). The authors would also like to acknowl-

edge the project “Multifunctional hybrid adsorbents for water purification” supported by the Swedish Research Council (Vetenskapsrådet), Dnr. 2018–2021.

## ■ REFERENCES

- (1) Chabukdhara, M.; Nema, A. K. Assessment of Heavy Metal Contamination in Hindon River Sediments: A Chemometric and Geochemical Approach. *Chemosphere* **2012**, *87*, 945–953.
- (2) Peng, C.; Meng, H.; Song, S.; Lu, S.; Lopez-Valdivieso, A. Elimination of Cr (VI) from Electroplating Wastewater by Electrodialysis Following Chemical Precipitation. *Sep. Sci. Technol.* **2005**, *39*, 1501–1517.
- (3) Ipeaiyeda, Ayodele Rotimi; Ia, R. A. Flame Atomic Absorption Spectrometric Determination of Heavy Metals in Aqueous Solution and Surface Water Preceded by Co-Precipitation Procedure with Copper (II) 8-Hydroxyquinoline. *Appl. Water Sci.* **2017**, *7*, 4449–4459.
- (4) Renu, M. A.; Agarwal, M.; Singh, K. Methodologies for Removal of Heavy Metal Ions from Wastewater: An Overview. *Interdiscip. Environ. Rev.* **2017**, *18*, 124–142.
- (5) Singh, N. B.; Nagpal, G.; Agrawal, S. Water Purification by Using Adsorbents: A Review. *Environ. Technol. Innov.* **2018**, *11*, 187–240.
- (6) Liu, Y.; Gao, G.; Vecitis, C. D. Prospects of an Electroactive Carbon Nanotube Membrane toward Environmental Applications. *Acc. Chem. Res.* **2020**, *53*, 2892–2902.
- (7) El Samrani, A. G.; Lartiges, B. S.; Villieras, F. Chemical Coagulation of Combined Sewer Overflow: Heavy Metal Removal and Treatment Optimization. *Water Res.* **2008**, *42*, 951–960.
- (8) Mortada, W. I. Recent Developments and Applications of Cloud Point Extraction: A Critical Review. *Microchem. J.* **2020**, *157*, No. 105055.
- (9) Babel, S.; Kurniawan, T. A. Low-Cost Adsorbents for Heavy Metals Uptake from Contaminated Water: A Review. *J. Hazard. Mater.* **2003**, *97*, 219–243.
- (10) Sarma, G. K.; Sen Gupta, S.; Bhattacharyya, K. G. Nanomaterials as Versatile Adsorbents for Heavy Metal Ions in Water: A Review. *Environ. Sci. Pollut. Res.* **2019**, *26*, 6245–6278.
- (11) Ricardo, A. I. C.; Abujaber, F.; Bernardo, F. J. G.; Mart’ín-Doimeadios, R. C. R.; Rios, A. Magnetic Solid Phase Extraction as a Valuable Tool for Elemental Speciation Analysis. *Trends Environ. Anal. Chem.* **2020**, *27*, No. e00097.
- (12) Lu, F.; Astruc, D. Nanomaterials for Removal of Toxic Elements from Water. *Coord. Chem. Rev.* **2018**, *356*, 147–164.
- (13) Thakur, V.; Sharma, E.; Guleria, A.; Sangar, S.; Singh, K. Modification and Management of Lignocellulosic Waste as an Ecofriendly Biosorbent for the Application of Heavy Metal Ions Sorption. *Mater. Today Proc.* **2020**, *32*, 608–619.
- (14) Trublet, M.; Scukins, E.; Carabante, I.; Rusanova, D. Competitive Sorption of Metal Ions on Titanium Phosphate Sorbent (TiP1) in Fixed-Bed Columns: A Closed-Mine Waters Study. *ACS Sustainable Chem. Eng.* **2019**, *7*, 8145–8154.
- (15) *Colloidal Silica Fundamentals and Applications*; Bergna, H.; Roberts, W., Eds.; CRC Press, 2005.
- (16) Da’na, E. Adsorption of Heavy Metals on Functionalized-Mesoporous Silica: A review. *Microporous Mesoporous Mater.* **2017**, *247*, 145–157.
- (17) Pierre, A. C. *Introduction to Sol-Gel Processing*, 2nd ed.; Springer Nature Switzerland, 2020 DOI: [10.1007/978-3-030-38144-8](https://doi.org/10.1007/978-3-030-38144-8).
- (18) Fulvio, P. F.; Pikus, S.; Jaroniec, M. Short-Time Synthesis of SBA-15 Using Various Silica Sources. *J. Colloid Interface Sci.* **2005**, *287*, 717–720.
- (19) Sanchez, C.; Julia, B.; Belleville, P.; Popall, M. Applications of Hybrid Organic – Inorganic Nanocomposites. *J. Mater. Chem.* **2005**, *15*, 3559–3592.
- (20) Zhao, D.; Huo, Q.; Feng, J.; Chmelka, B. F.; Stucky, G. D. Nonionic Triblock and Star Diblock Copolymer and Oligomeric Surfactant Syntheses of Highly Ordered, Hydrothermally Stable, Mesoporous Silica Structures. *J. Am. Chem. Soc.* **1998**, *120*, 6024–6036.

- (21) Zhao, T.; Elzatahry, A.; Li, X.; Zhao, D. Single-Micelle-Directed Synthesis of Mesoporous Materials. *Nat. Rev. Mater.* **2019**, *4*, 775–791.
- (22) Li, J.; Wang, L.; Qi, T.; Zhou, Y.; Liu, C.; Chu, J.; Zhang, Y. Different N-Containing Functional Groups Modified Mesoporous Adsorbents for Cr(VI) Sequestration: Synthesis, Characterization and Comparison. *Microporous Mesoporous Mater.* **2008**, *110*, 442–450.
- (23) Vunain, E.; Mishra, A.; Mamba, B. Dendrimers, Mesoporous Silicas and Chitosan-Based Nanosorbents for the Removal of Heavy-Metal Ions: A Review. *Int. J. Biol. Macromol.* **2016**, *86*, 570–586.
- (24) Liu, S.; Cui, H.; Li, Y.; Yang, A.; Zhang, J.; Zhong, R.; Zhou, Q.; Lin, M.; Hou, X. Bis-Pyrazolyl Functionalized Mesoporous SBA-15 for the Extraction of Cr(III) and Detection of Cr(VI) in Artificial Jewelry Samples. *Microchem. J.* **2016**, *131*, 130–136.
- (25) Benhamou, A.; Baudu, M.; Derriche, Z.; Basly, J. P. Aqueous Heavy Metals Removal on Amine-Functionalized Si-MCM-41 and Si-MCM-48. *J. Hazard. Mater.* **2009**, *171*, 1001–1008.
- (26) Gupta, R.; Kumar, S.; Deo, D. Selective Adsorption of Toxic Heavy Metal Ions Using Guanine-Functionalized Mesoporous Silica [SBA-16-g] from Aqueous Solution. *Microporous Mesoporous Mater.* **2019**, *288*, No. 109577.
- (27) Faghihian, H.; Naghavi, M. Synthesis of Amine-Functionalized MCM-41 and MCM-48 for Removal of Heavy Metal Ions from Aqueous Solutions Synthesis of Amine-Functionalized MCM-41 and MCM-48 for Removal of Heavy Metal Ions from Aqueous Solutions. *Sep. Sci. Technol.* **2014**, *49*, 37–41.
- (28) Kruk, M.; Jaroniec, M.; Ko, C. H.; Ryoo, R. Characterization of the Porous Structure of SBA-15. *Chem. Mater.* **2000**, *12*, 1961–1968.
- (29) Javadian, H.; Vahedian, P.; Toosi, M. Adsorption Characteristics of Ni(II) from Aqueous Solution and Industrial Wastewater onto Polyaniline/HMS Nanocomposite Powder. *Appl. Surf. Sci.* **2013**, *284*, 13–22.
- (30) Wei, J. Aqueous Cu (II) Ion Adsorption by Amino-Functionalized Mesoporous Silica KIT-6. *RSC Adv.* **2020**, *10*, 20504–20514.
- (31) Bruin-dickason, C. N.; De; Jaworski, A.; Chen, J.; Budnyak, T.; Slabon, A. Glycine-Functionalized Silica as Sorbent for Cobalt (II) and Nickel (II) Recovery. *Appl. Surf. Sci.* **2020**, *530*, No. 147299.
- (32) Knepper, T. P. Synthetic Chelating Agents and Compounds Exhibiting Complexing Properties in the Aquatic Environment. *TrAC, Trends Anal. Chem.* **2003**, *22*, 708–724.
- (33) Kolodyńska, D. Application of a New Generation of Complexing Agents in Removal of Heavy Metal Ions from Different Wastes. *Environ. Sci. Pollut. Res.* **2013**, *20*, 5939–5949.
- (34) Zhang, K.; Dai, Z.; Zhang, W.; Gao, Q.; Dai, Y.; Xia, F.; Zhang, X. EDTA-Based Adsorbents for the Removal of Metal Ions in Wastewater. *Coord. Chem. Rev.* **2021**, *434*, No. 213809.
- (35) Dudarko, O. A.; Zub, Y. L.; Dabrowski, A.; Barczak, M. Polysiloxane Xerogels with a Bifunctional Surface Layer Containing O/N, O/S, S/N, and S/S Donor Centers. *Russ. J. Appl. Chem.* **2008**, *81*, 114–122.
- (36) Pandey, L. M. Surface Engineering of Nano-Sorbents for the Removal of Heavy Metals: Interfacial Aspects. *J. Environ. Chem. Eng.* **2020**, *9*, No. 104586.
- (37) Zaitsev, V. N.; Kostenko, L. S.; Kobylinskaya, N. G. Acid-Base Properties of Silica-Based Ion-Exchanger Having Covalently Bonded Aminodi(Methylphosphonic) Acid. *Anal. Chim. Acta* **2006**, *565* (). DOI: 10.1016/j.aca.2006.02.030.
- (38) Costa, J. A. S.; Paranhos, C. M. Mitigation of Silica-Rich Wastes: An Alternative to the Synthesis Eco-Friendly Silica-Based Mesoporous Materials. *Microporous Mesoporous Mater.* **2020**, *309*, No. 110570.
- (39) Brunauer, S.; Emmett, P. H.; Telle, E. Adsorption of Gases in Multimolecular Layers. *J. Am. Chem. Soc.* **1938**, *60*, 309–319.
- (40) Barrett, E. P.; Joyner, L. G.; Halenda, P. P. The Determination of Pore Volume and Area Distributions in Porous Substances. I. Computations from Nitrogen Isotherms. *J. Am. Chem. Soc.* **1951**, *73*, 373–380.
- (41) Sing, K. S. W. Reporting Physorption Data for Gas/Solid Systems with Special Reference to the Determination of Surface Area and Porosity. *Int. UNION PURE Appl. Chem.* **1982**, *54*, 2201–2218.
- (42) Da-zhou, Z.; Shu-bo, J.; Jia-ning, X. U.; Hong, Y.; Wei, Z. Recycle Adsorption of Cu<sup>2+</sup> on Amine-Functionalized Mesoporous Silica Monolithic. *Chem. Res. Chin. Univ.* **2013**, *29*, 793–797.
- (43) Manuscript, A. Cooperative Acid-Base Bifunctional Ordered Porous Solids in Sequential Multi-Step Reactions: MOF vs. Mesoporous Silica. *Catal. Sci. Technol.* **2020**, 1796–1802.
- (44) Smith, R. M.; Martell, A. E. Critical Stability Constants, Enthalpies and Entropies for the Formation of Metal Complexes of Aminopolycarboxylic Acids and Carboxylic Acids. *Sci. Total Environ.* **1987**, *64*, 125–147.
- (45) Shao, P.; Liang, D.; Yang, L.; Shi, H. Evaluating the Adsorptivity of Organo-Functionalized Silica Nanoparticles Towards Heavy Metals: Quantitative Comparison and Mechanistic Insight. *J. Hazard. Mater.* **2019**, *387*, No. 121676.
- (46) Giles, C. H.; Smith, D.; Huitson, A. A General Treatment and Classification of the Solute Adsorption Isotherm. I. Theoretical. *J. Colloid Interface Sci.* **1974**, *47*, 755–765.
- (47) Pearson, R. G. Hard and Soft Acids and Bases. *J. Am. Chem. Soc.* **1963**, *85*, 3533–3539.
- (48) Da'na, E.; Sayari, A. Adsorption of Heavy Metals on Amine-Functionalized SBA-15 Prepared by Co-Condensation: Applications to Real Water Samples. *Desalination* **2012**, *285*, 62–67.
- (49) Repo, E.; Warchol, J. K.; Bhatnagar, A.; Sillanpää, M. Heavy Metals Adsorption by Novel EDTA-Modified Chitosan-Silica Hybrid Materials. *J. Colloid Interface Sci.* **2011**, *358*, 261–267.
- (50) Yuh-Shan, H. Citation Review of Lagergren Kinetic Rate Equation on Adsorption Reactions. *Scientometrics* **2004**, *59*, 171–177.
- (51) Ho, Y. S.; M, G. Pseudo-Second Order Model for Sorption Processes. *Process Biochem.* **1999**, *34*, 451–465.
- (52) Weber, W. J.; Morris, J. C. Adsorption in Heterogeneous Aqueous Systems. *J. Am. Water Works Assoc.* **1964**, *56*, 447–456.
- (53) Herschy, R. W. Water Quality for Drinking: WHO Guidelines. *Encyclopedia Earth Sci. Ser.* **2012**, 876–883.
- (54) Linnik, P. N.; Zhezherya, V. A.; Linnik, R. P.; Ignatenko, I. I.; Zubenko, I. B. Metals in Surface Water of Ukraine: The Migration Forms, Features of Distribution between the Abiotic Components of Aquatic Ecosystems, and Potential Bioavailability. *Russ. J. Gen. Chem.* **2015**, *85*, 2965–2984.